Quaternary Science Reviews 368 (2025) 109555

Contents lists available at ScienceDirect

Quaternary Science Reviews

journal homepage: www.elsevier.com/locate/quascirev

New palaeoecological insights for the early human occupation in Europe: amphibians and reptiles from the Early Pleistocene of Pirro Nord 13 (Apricena, southern Italy)

Christian Sánchez-Bandera [a,b,*], Hugues-Alexandre Blain [a,b], Josep Francesc Bisbal-Chinesta [a,b], Ana Fagoaga [c,d], Marco Pavia [e,f], Massimo Delfino [e,g]

[a] IPHES-CERCA, Institut Català de Paleoecologia Humana i Evolució Social, Zona Educacional 4, Campus Sescelades URV (Edifici W3), 43007, Tarragona, Spain
[b] Departament d'Història i Història de l'Art, Universitat Rovira i Virgili, Avinguda de Catalunya 35, 43002, Tarragona, Spain
[c] PVC-GIUV (Palaeontology of Cenozoic Vertebrates Research Group), Àrea de Paleontologia, Universitat de València, Dr. Moliner 50, E-46100, Valencia, Spain
[d] Museu Valencià D'Història Natural, L'Hort de Feliu, P.O. Box 8460, Alginet, E-46018, Valencia, Spain
[e] Dipartimento di Scienze Della Terra, Università di Torino, Via Valperga Caluso 35, 10125, Torino, Italy
[f] Research and Exhibitions, Iziko Museums of South Africa, 25 Queen Victoria Street, Cape Town, 8001, South Africa
[g] Institut Català de Paleontologia Miquel Crusafont (IPC-CERCA), Edifici ICTA-ICP, c/Columnes s/n, Campus de la UAB, Cerdanyola del Vallès, 08193, Barcelona, Spain

ARTICLE INFO

Handling editor:

Keywords:
Early Pleistocene
Amphibia
Reptilia
Palaeoclimatology
Palaeoenvironment
Early hominins

ABSTRACT

The Early Pleistocene site of Pirro Nord 13, dated between 1.6 and 1.3 Ma, is one of the fissures of the karstic complex of the Pirro Nord quarry (Apricena, Foggia, southern Italy), a well-known locality for its rich and well-preserved palaeontological record. Among the identified sites, Pirro Nord 13 has a particular importance because it documents the largest amount of human evidence at Pirro Nord and represents one of the earliest human records of western Europe. In this study, we fully described for the first time the fossil amphibians and reptiles from Pirro Nord 13, which are hosted at the Museo di Geologia e Paleontologia collections (MGPT-PU) at Torino University (Turin, Italy), and used them to perform quantitative palaeoecological reconstructions. The resulted herpetofaunal assemblage is composed by a total of 13 species: four anurans (*Pelobates syriacus*, *Bufotes viridis* gr., *Bufo* gr. *B. bufo* and *Pelophylax* cf. *esculentus/ridibundus*), three chelonians (*Testudo hermanni*, *Emys orbicularis* and *Mauremys* sp.), three lizards (cf. *Podarcis* sp., *Lacerta* s.l. and *Blanus* sp.), and three snakes (*Natrix* gr. *N. natrix*, *Coronella* cf. *C. austriaca*, and *Zamenis* gr. *Z. longissimus*). In order to address the palaeoecological reconstruction, we applied the Mutual Ecogeographic Range method with the Uncertain Distribution Area-Occupied Distribution Area technique to obtain temperature and precipitation estimates, and the Habitat Weighting method to infer the surrounding environment. The Pirro Nord 13 climate (USs A-C) was reconstructed as cold and semi-humid, with lower temperatures (−4.4 °C) and similar precipitations (+45 mm) levels to the present-day, but with a less pronounced seasonality. The inferred landscape was reconstructed as dominated by open environments primarily composed of open-dry habitats (29.59 %), however with the presence of woodland (19.12 %) along water bodies or temporary swamps (21.82 %). The results obtained provide significant insights into the ecological tolerance of early hominins, suggesting that they were able to cope with challenging climatic and environmental conditions, and contribute to our understanding of their distribution and the delays observed in their dispersals across the European continent.

1. Introduction

Climate has been widely identified as one of the primary factors potentially affecting early hominin evolution and their dispersal into Eurasia, together with other factors such as technological innovation (e.g., Agustí et al., 2009, 2018; deMenocal, 2011; Blain et al., 2021; Margari et al., 2023; Sánchez-Bandera et al., 2020, 2023; Timmermann et al., 2022, 2024). Therefore, a study of the ecological circumstances

* Corresponding author. Zona Educacional 4, Campus Sescelades URV (Edifici W3), 43007, Tarragona, Spain.
E-mail address: csanchezbandera@iphes.cat (C. Sánchez-Bandera).

https://doi.org/10.1016/j.quascirev.2025.109555
Received 27 February 2025; Received in revised form 29 July 2025; Accepted 29 July 2025
Available online 9 August 2025

under which the first human dispersals on the European continent took place would provide substantial insights concerning the capabilities, constraints and behavioural patterns of these early populations.

In this context, the Early Pleistocene site of Pirro Nord 13 is of particular significance, given its rich and well-preserved palaeontological assemblage, and for presenting one of the earliest hominin evidences in Europe. This site is positioned in time and space between the "eastern" early hominin sites of Korolevo, Ukraine (Garba et al., 2024), Grăunceanu, Romania (Curran et al., 2025), Kocabaş, Turkey (Vialet et al., 2018), and Dmanisi, Georgia (Gabunia et al., 2000), with chronologies comprised between ca. 2.0 and 1.4 Ma, and the "western" early hominin sites such as Le Vallonet, France (Cauche, 2022), Pont-de-Lavaud, France (Despriée et al., 2018), Sima del Elefante TE7 and TE9c, Spain (Carbonell et al., 2008; Huguet et al., 2025), Barranco León, Spain (Toro-Moyano et al., 2013), or Fuente Nueva 3, Spain (Barsky et al., 2022), with somewhat younger chronologies comprised between ca.1.4 and 1.1 Ma. Consequently, a comprehensive understanding of the climatic and environmental conditions of Pirro Nord 13 is essential for unravelling early European dispersals and disruptions, and for a more precise characterisation of their ecological niche.

The aim of the present work is to provide quantitative palaeoecological reconstructions for the Early Pleistocene site of Pirro Nord 13 based on its fossil amphibian and reptile assemblage, with the purpose of providing further insights into the ecological tolerance of the early hominins.

1.1. Pirro Nord 13

The Pirro Nord 13 site (hereafter referred to as PN13) is one of the karst fissures found in the Pirro Nord quarry (locality also known as Cava Pirro or Cava Dell'Erba), located at the northwestern margin of the Gargano promontory, in the municipality of Apricena (Foggia, southern Italy; the coordinates of the site in WGS84 are 41.801667, 15.384722; Fig. 1A and B). The area consists of a system of uplifted Jurassic and Cretaceous limestones in which a karst system was first activated during the Late Miocene in the Apricena horst.

This karst system is distinguished by its intricate network of fissures and sinkholes, which are believed to represent a single karst cycle (Pavia et al., 2012). Over 30 of these fissures have delivered a rich assemblage of large and small vertebrate faunas. Among them, however, only a few have yielded lithic artefacts, namely PN10, PN13 and PN21 (Arzarello et al., 2009), with PN13 site presenting the richest collection.

More than 500 Oldowan lithic artefacts (Arzarello et al., 2015) have been recovered in PN13 (Arzarello et al., 2015), which, together with the butchering traces and breaking patterns found on large-mammal bones (Cheheb et al., 2019; Berruti and Arzarello, 2020), represent one of the earliest hominin occurrences in Western Europe (Arzarello et al., 2007, 2012, 2015).

1.1.1. Stratigraphy and deposit formation

The PN13 deposit is more than 4 m thick and is characterised by a sandy loam matrix with clasts and blocks of local lithology, exhibiting a

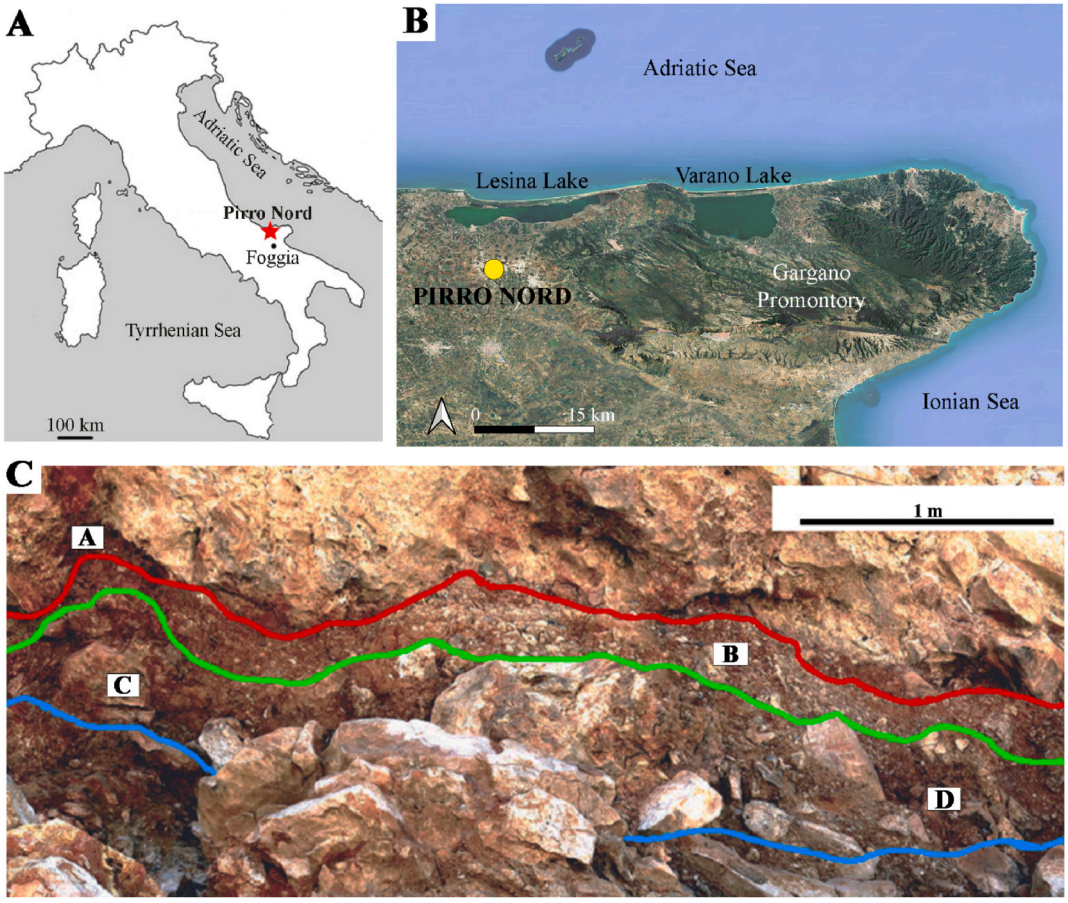

Fig. 1. Geographic location and stratigraphic schema of the Early Pleistocene site of Pirro Nord 13. **A**, Geographic location of the PN13 site in the Apennine Peninsula, inside the province of Foggia (Puglia, southern Italy); **B**, Detailed geographic location of the PN13 site inside the municipality of Apricena, and close to the Gargano Promontory; **C**, Stratigraphy of PN13. Labels indicate the Stratigraphic Units (SU) and lines mark their respective bases. SU A: thin sandyclayey layer that covers the underlying units; SU B: disorganised structure of numerous sub-rounded less than decimetric clasts in sandy, muddy matrix; SU C: disorganised structure of varying sizes of decametric clasts and boulders in a brown-green muddy sand matrix; and SU D: same as SU C but with larger boulders and common sandy lenses, which are sometimes structured in thin layers with alterations of sand and mud (modified from Cheheb et al., 2019). Abbreviations: km = kilometres; m = metres.

chaotic arrangement and distribution. Based on their lithological and sedimentary composition, four sedimentary units (SUs) have been distinguished, from unit A to unit D (Fig. 1C). Unit A consists of a thin sandy-clayey layer that covers the underlying units. Units B to D are composed of sandy loam sediment among limestone and calcarenite cobbles and boulders, which show poor sorting and variable size and roundness. Units C and D show an abrupt increase in the number and dimension of clasts and large blocks and a significant increase in the number of fossil and lithic artefacts as well (Giusti and Arzarello, 2016; Berruti and Arzarello, 2020).

The formation of the deposit has been analysed in several studies, considering the stratigraphy and the taphonomic processes (e.g. Bagnus, 2011; Berruti, 2017; Giusti and Arzarello, 2016). These studies suggest that PN13 was initially formed by the collapse of the top and walls of a karst fissure, followed by a deposition of sediment and large boulders due to mudflows or earthflows produced by rainfall or other weather-related events. Animals that died or were deposited near the karst sinkhole, together with lithic artefacts and large blocks of calcarenite and limestone, were subsequently transported into the fissure by the action of flows caused by heavy rainfall, and rapidly buried.

An applied set of spatial analyses (Giusti and Arzarello, 2016), in conjunction with geochemical analyses and geoarchaeological revision of the site (Karampatsou, 2017), suggested that the formation of SUs B, C, and D was the result of a gravitational selection of the chaotic materials carried into the fissure during one or more of the above-mentioned mud flow or earth flow events.

Considering this geomorphological and stratigraphic setting, the depositional processes, and the faunal and lithic artefact remains, PN13 is considered as a homogeneous assemblage, with no evidence of post-depositional reworking and mixing of the sedimentary deposit (Giusti and Arzarello, 2016; Cheheb et al., 2019; Berruti and Arzarello, 2020).

1.1.2. Faunal community of PN13

The large-mammal assemblage of PN13 is principally composed of herbivores (*Mammuthus meridionalis*, *Stephanorhinus* cf. *hundsheimensis*, *Bison (Eobison) degiulii*, *Equus altidens*, *Pseudodama* cf. *farnetensis*), and carnivores (*Pachycrocuta brevirostris*, *Ursus etruscus*, *Canis mosbachensis*, and *Meles* sp.) (Cheheb et al., 2019).

Regarding the small-mammals, it is represented by bats (*Miniopterus shreibersii*, *Myotis* gr. *My. myotis-blithii*, *Rhinolophys* gr. *R. euryale-mehelyi*, and *R. ferrumequinum*), insectivores (*Crocidura kornfeldi*, *Asoriculus* sp., *Sorex* sp., *Erinaceus praeglacialis*, and *Talpa* gr. *T. minor-caeca*), and rodents (*Allophaiomys* cf. *ruffoi*, *Apodemus* sp., *Eliomys* cf. *intermedius*, and *Hystrix refossa*). Among the identified taxa, the assemblage is clearly dominated by the rodent *A.* cf. *ruffoi* (López-García et al., 2015; Berto et al., 2024).

1.1.3. Chronology

The chronology of PN13 is based primarily on biochronological correlations of both large and small mammal assemblage, which indicate an age confined between 1.6 and 1.3 Ma. The large-mammal assemblage gives name to the Pirro Nord Faunal Unit (FU), the last FU of the late Villafranchian mammal age in the Italian biochronological scale (De Giuli et al., 1986; Abbazzi et al., 1996; Gliozzi et al., 1997; Masini and Sala, 2007, 2011). Concerning rodents, the association documented at PN13 suggests an age roughly ranging between 1.6 and 1.3 Ma (López-García et al., 2015; Berto et al., 2024). PN13 is considered to be similar in age as Venta Micena (Agustí et al., 2010; Duval et al., 2011), and older (more archaic) than the *Allophaiomys lavocati* associations from Barranco León (Toro-Moyano et al., 2013), Fuente Nueva 3 (Duval et al., 2012), and Sima del Elefante (levels TE9–TE14, Carbonell et al., 2008; Cuenca-Bescós et al., 2013). PN13 has thus been included in the Early Biharian mammal age, within the *Mimomys savini - Mimomys pusillus* zone (Sala and Masini, 2007; López-García et al., 2015).

Recent dating analyses from PN13, based on radiometric approaches (Duval et al., 2024), differ from the biochronological evidence. These analyses provide an age clustering around 0.8 Ma. However, these novel chronological data are yet to be fully interpreted (Berto et al., 2024), and are out of the scope of the present study.

2. Material and methods

2.1. Amphibian and reptile assemblage

The fossil herpetological remains from PN13 used in this study come from the collections of the Museo di Geologia e Paleontologia (MGPT-PU) of the Torino University (Turin, Italy). The fossil assemblage mainly consists of disarticulated elements collected by water-screening of the sediments obtained during the 2007 and 2008 fieldwork seasons. Sediments were water-screened using superimposed 1 mm and 0.5 mm mesh screens. The material was sorted and studied at the Dipartimento di Scienze della Terra of the Torino University (Turin, Italy) and was subsequently housed at the MGPT-PU.

For the osteological comparisons, we used the dry skeleton collections of the Institut Català de Paleoecologia Humana i Evolució Social (IPHES-CERCA, Tarragona), Dipartimento di Scienze della Terra of the Università degli Studi di Torino (Massimo Delfino Herpetological Collection, MGPT-MDHC), and the Hungarian Natural History Museum (HNHM, Budapest). The taxonomic nomenclature follows Speybroeck et al. (2020).

We quantified the fossils following the Minimum Number of Elements (MNE) and Minimum Number of Individuals (MNI) methods. The MNE corresponds to the number of anatomical elements, without considering fragments or partial bones. To assess the MNI we counted the most represented element divided by the number of present elements in a living specimen (i.e. considering laterality when possible). In the case of anurans, sex has also been used for humeri (unless for *Pelobates*, where this pattern is absent). In the case of snakes, which typically are only represented by vertebrae, we assessed the MNI by considering, when possible, the relative size of the trunk vertebrae (i.e. centrum length).

We took the pictures using an AM4115TL Dino-Lite Edge Digital microscope, using the DinoCapture 2.0 software, and then processed them with the Helicon Focus 3.10 freeware.

2.2. Palaeoclimatic reconstruction

In order to reconstruct the palaeoclimatic scenario for Pirro Nord 13 site, we applied the Mutual Ecogeographic Range (MER) method (Blain et al., 2016a) with the Uncertain Distribution Area-Occupied Distribution Area (UDA-ODA) discrimination technique (Fagoaga et al., 2019) to its herpetofaunal assemblage. The MER method consists of extrapolating mean values of climatic parameters of the geographical regions currently displaying the same species assemblage as the fossil site (Blain et al., 2016a). This method is based on presence/absence (and not abundance) and so is not particularly affected by taphonomic biases and/or over-representation of some species. For its application, it assumes niche conservatisms, that is, fossil representatives of the extant species have the same climatic tolerances and preferences as their living counterparts (Jackson and Overpeck, 2000; Jackson and Williams, 2004). Nevertheless, the application of this method suggests avoiding species whose distribution is strongly affected by perturbing non-climatic variables (i.e. human pressure). To determine the current spatial distribution of European amphibians and reptiles, we used the data from Sillero et al. (2014), represented in a geographic coordinate system (WGS 84 datum) with a 50 × 50 km square grid. In cases where species-level identification was not achieved (i.e., *Mauremys* sp., cf. *Podarcis* sp., and *Lacerta* s.l.), all the extant species belonging to the corresponding genus were taken into consideration. We have not considered *Blanus* sp. in the analysis as it has not been possible to identify the fossils at a species level, and the two extant representatives of the genus (i.e., *Bl. cinereus* complex and *Bl. strauchi* complex) exhibit a

relict and disjunctive distribution, with a widely fragmented range (see Delfino, 1997; Sindaco et al., 2014). However, the climatic requirements of existing populations can be compared with the quantitative results.

For its part, the UDA-ODA discrimination technique represents a refinement of the MER method based on the implementation of Geographic Information Systems (GIS). This technique incorporates the species ecological requirements to create more accurate distribution areas (ODAs), which are then used in the overlapping process. In contrast to the coarse-grained distributions proposed by many atlases, this approach provides a more precise and accurate representation of the distribution of species (Fagoaga et al., 2019; Marquina-Blasco et al., 2022; Yeshurun et al., 2024). Additionally, this procedure facilitates the management of large datasets and improves the reproducibility of the results.

In our study, we used the upper elevation limit of *Emys orbicularis* (1200 m, Pleguezuelos et al., 2002) to more precisely delimit the species overlapping area by removing those areas exceeding this elevation limit. This boundary represents the maximum altitudinal limit for all species in the assemblage (see Table S1 for details).

From the final overlapping area, we calculated annual (MAT, mean annual temperature; MAP, mean annual precipitation) and monthly climatic parameters (mean monthly temperature; MTW, mean temperature of warmest month; MTC, mean temperature of coldest month; mean monthly precipitation) using the data from WorldClim 2.1, with a 30 arcsecond resolution grid (Fick and Hijmans, 2017). The same climatic parameters were calculated for the Pirro Nord 13 site location nowadays (1970–2000) within a 5 km^2 area. We processed the datasets using the free software QGIS 3.22.14.

To measure aridity, we used the Gaussen, Lautensach-Meyer, Dantin-Revenga and De Martonne indexes (see for example Muñoz-Delgado, 2003). The Gaussen index ($P < 2 \times T$) regards a dry month as occurring when its pluviometric level (P), measured in mm, is less than twice the value of the average temperature in °C for that month (T). The Lautensach-Meyer index regards a dry month if its pluviometric level (P), measured in mm, is < 30 mm. The Dantin-Revenga index is calculated as 100 x MAT/MAP, and the De Martonne aridity index as MAP/(MAT + 10).

2.3. Palaeoenvironmental reconstruction

For the palaeoenvironmental reconstruction we used the Habitat Weighting method (adapted by Blain et al., 2008 for herpetofauna). This method is based on distributing each amphibian and reptile species in the habitat(s) in which they can be found today, and estimating the representation of these different habitats around the site in the past based on the MNI per taxon (Table 1).

We divided the habitats into five categories: *Open Dry*: environments with minimal vegetation or vegetation of low height and subject to seasonal changes in humidity, especially during the summer drought; *Open Humid*: wet areas with low perennial and dense vegetation that remains wet throughout the year; *Woodland*: environments with greater plant cover reaching comparatively greater heights, from medium scrublands to closed forests, including the margin of these areas; *Rocky and/or Stony*: open environments with low or scarce vegetation, nutrient poor substrate and an abundance of emerged rock and stones; *Water Edge*: aquatic and peri-aquatic environments, permanent or temporary bodies of water and their immediate surrounding areas, with hydrophilic and hygrophilous vegetation (Cuenca-Bescós et al., 2005).

Each species was assigned a maximum possible score of 1.00, which was distributed according to its habitat preferences. If a species occurred in more than one habitat category, the corresponding scores were proportional to its total habitat preferences. We have not considered family-level groups or groups containing species with contrasting ecological preferences (such as lacertids).

Distribution by habitats of the species represented in PN13 (Table 2) mainly followed Blain et al. (2019), completed for *Pelobates syriacus* and *Blanus* sp. following their ecological requirements (Arnold and Burton, 1978; Pleguezuelos et al., 2002; Sindaco et al., 2009, 2014).

2.4. Fossil assemblages and species interrelationship analyses

A total of 26 palaeontological sites from the Pirro Nord locality, which document herpetological records, have been selected for the analyses. Together with PN13, we have used these sites to examine the interrelationship between their assemblages and the species documented. These sites are: PN1, PN2, PN5, PN5b, PN6, PN9, PN11, PN12, PN15, PN16, PN17, PN18, PN22err, PN22 in posto, PN22bis, PN24,

Table 1
Taxonomic list of the amphibian and reptiles represented in the Early Pleistocene site of Pirro Nord 13 (Apricena, southern Italy), by Minimum Number of Elements (MNE) and by Minimum Number of Individuals (MNI). The 'X' symbol in SU D refers to the documentation of *Pelobates syriacus* attested by Blain et al. (2016b). *In the PN13 assemblage, fossil material recovered during the 2007's excavation campaign that has not been assigned to any of the subsequent described SUs is also considered. Abbreviation: SU = Stratigraphic Unit.

Taxonomic list	SU A		SU B		SU C		SU D		PN13*	
	MNE	MNI	MNE	MNI	MNE	MNI	MNE	MNI	MNE	MNI
Pelobates syriacus	11	2	14	2	1	1	X		31	3
Bufotes viridis gr.	45	7	49	7	14	5	3	1	131	21
Bufo gr. *B. bufo*			9	1	6	2			19	3
Bufonidae indet.	11		18		3				47	
Pelophylax cf. *esculentus/ridibundus*	10	2	13	3	3	2			25	6
Anura indet.	57		41		11				129	
Testudo hermanni	3	1	27	4					116	6
Emys orbicularis	4	1	1	1					18	2
Mauremys sp.			1	1					8	2
Freshwater turtle indet.			1						6	
Testudines indet.	3		10						134	
cf. *Podarcis* sp.	42	12	48	13	3	2			98	29
Lacerta s.l.	3	2	6	1	5	1			16	3
Blanus sp.	11	2	13	5	1	1			27	3
Lacertilia indet.	2		2						7	
Natrix gr. *N. natrix*	11	5	47	7	11	5			92	7
Coronella cf. *C. austriaca*	24	2	10	3	3	2			28	7
Zamenis gr. *Z. longissimus*	39	8	86	6	19	5			186	11
Colubridae indet.	15		89		28		1		183	
Serpentes indet.	38		136		27				255	
TOTAL	**329**	**44**	**621**	**54**	**135**	**26**	**4**	**1**	**1556**	**103**

Table 2
Distribution by habitat of the amphibian and reptiles represented in the Early Pleistocene site of Pirro Nord 13 (Apricena, southern Italy). Values for habitat weightings are in percentages (%). Abbreviations: OD = Open Dry; OH = Open Humid, W = Woodland, R/S = Rocky and/or Stony, WE = Water Edge.

Taxonomic list	Habitat distribution				
	OD	OH	W	R/S	WE
Pelobates syriacus	0.7			0.1	0.2
Bufotes viridis gr.	0.65			0.25	0.1
Bufo gr. *B. bufo*	0.1	0.3	0.4		0.2
Bufonidae indet.	x	x	x	x	x
Pelophylax cf. *esculentus/ridibundus*					1
Anura indet.	x	x	x	x	x
Testudo hermanni	0.5		0.2	0.3	
Emys orbicularis					1
Mauremys sp.					1
Freshwater turtle indet.	x	x	x	x	x
Testudines indet.	x	x	x	x	x
cf. *Podarcis* sp.	x	x	x	x	x
Lacerta s.l.	0.5		0.1	0.4	
Blanus sp.	0.45	0.1	0.45		
Lacertilia indet.	x	x	x	x	x
Natrix gr. N. *natrix*		0.5	0.25		0.25
Coronella cf. *C. austriaca*		0.5	0.25	0.25	
Zamenis gr. *Z. longissimus*		0.3	0.6		0.1
Colubridae indet.	x	x	x	x	x
Serpentes indet.	x	x	x	x	x

PN24b, PN25, PN26, PN30, PN32, PN34err, PN34a, PN34c, PN34d and PN35 (Table S2). Their herpetofaunal assemblages have been reported and described by Delfino (1996), Delfino and Bailon (2000), and Delfino and Atzori (2013). We have included the assemblages into a data matrix, using binary presence-absence, to analyse the relationship between them on basis of their herpetofaunal assemblages (Table S3). We have excluded the mono-specific citations of chelonians (e.g., *Mauremys* sp. from PN11 spb and *Testudo hermanni* from PN22 sacca) from the data matrix, to avoid statistical deviations, although we included in the subsequent discussion.

To analyse the interrelationships between the different species that have been found in the selected sites and their possible biogeographic, palaeoenvironmental and/or chronostratigraphic implications, we applied the method of hierarchical clustering with binary presence/absence data using the Jaccard similarity index together with the "unweighted pair-group average" to the data matrix, which results in the union in the dendrogram of different groups based on the average distance between their members (Hammer et al., 2001). This method allows to relate the different species through the documented concurrences, that is, the joint appearance of them in the same palaeontological site, generating clades according to the proximity relationship. The use of a hierarchical method generates a cluster from the data matrix that must be validated, due to the possible inclusion of distortions in the original relationships. For this purpose, we used the cophenetic correlation coefficient, through which is observed the relationship between the resulting dendrogram and the original proximity matrix and whose value must be as high as possible, being always less than or equal to 1 (Sokal and Rohlf, 1962).

We then used the correspondence analysis (CA) to further examine the relationship between the different herpetofaunal associations of Pirro Nord and their species, and to infer possible palaeoecological trends within its fossil herpetofaunal record. This method is recommended for comparison between assemblages (assigned to the columns in the matrix) with the species they include (assigned to the rows) in an equivalent way (Greenacre, 2010). The objective of this procedure was to delineate the relationships of proximity between taxa of different associations, grouping them closely in contrast to the more atypical taxa, which will appear in an eccentric position with respect to the rest of the set. Both analyses have shown great coherence in the synchronic and diachronic regional studies of the palaeoherpetological record (Bisbal-Chinesta and Blain, 2018). For these statistical approaches we used the Paleontological Statistics program (PAST 4.17) (Hammer et al., 2001).

2.5. Statistical analyses

To ascertain the reliability of the climatic and environmental comparisons between the palaeoecologically reconstructed deposits of Pirro Nord (i.e. PN1, PN2, PN5, PN5b, PN9, PN11, PN12, PN16, and PN17; analysed by Blain et al., 2019) and PN13 (this study), which present herpetofaunal assemblages of differing sample size (see Table S3), we statistically standardised the samples. To do this, we elaborated rarefaction (interpolation) and prediction (extrapolation) curves with Hill numbers method (Colwell et al., 2012; Chao et al., 2014). This method also allowed us to compare the species diversity, which incorporates species richness and the relative abundance of each species, between assemblages. The curves were drawn based on the integrated sample-size and sample-coverage analytic approaches (Chao and Jost, 2012). Hill numbers include the three most widely used species diversity measures: species richness ($q = 0$), Shannon diversity ($q = 1$) and Simpson diversity ($q = 2$), and are increasingly dominated by the frequencies of the more common species. Finally, we used the bootstrap method to construct 95 % confidence intervals for the expected interpolated and extrapolated curves (Chao et al., 2014). We used iNEXT (iNterpolation/EXTrapolation) online freeware application R-based version (Chao et al., 2016) to process the statistical analyses.

3. Results

The PN13 assemblage hosted at MGPT-PU includes a total of 1556 amphibian and reptile fossil bones (MNE), corresponding to 103 individuals (MNI). The resulting taxonomic list consist of 13 species (Table 1): four anurans (*Pelobates syriacus*, *Bufotes viridis* gr., *Bufo* gr. *B. bufo* and *Pelophylax* cf. *esculentus/ridibundus*), three chelonians (*Testudo hermanni*, *Emys orbicularis* and *Mauremys* sp.), three lizards (cf. *Podarcis* sp., *Lacerta* s.l. and *Blanus* sp.), and three snakes (*Natrix* gr. *N. natrix*, *Coronella* cf. *C. austriaca*, and *Zamenis* gr. *Z. longissimus*).

3.1. Systematic palaeontology

Class Amphibia Linnaeus, 1758
Order Anura Duméril, 1805.

Toads and frogs are represented in PN13 by 382 elements (NR; Table 1), documenting 33 individuals (MNI; Table 1), and belonging to four species. We have attributed 129 elements at the Order level only because of their incompleteness or because of a lack of associability with more diagnostic elements from the same sample (2 squamosal, 5 articulars s.l., 10 vertebrae, 2 urostyles, 1 scapula, 6 humeri, 13 radioulnae, 9 ilia, 5 femora, 53 tibiofibulae, 8 tarsal bones, and 15 phalanges).

Family Pelobatidae Bonaparte, 1850.
Genus *Pelobates* Wagler, 1830.
Pelobates syriacus Boettger, 1889 – Eastern Spadefoot Toad.
(Fig. 2A–G)

Material: 7 maxillae, 2 sphenethmoids, 2 scapulae, 1 atlas, 7 vertebrae, 2 sacra, 5 humeri, and 5 ilia.

Description: We recovered seven maxillae from PN13. Most are fragmentary, except for two more nearly complete specimens. The most complete maxilla (Fig. 2A) preserves the central part of the element, and an anteriorly incomplete lamina anterior. Except for a narrow and relatively smooth strip along the ventrolateral edge of the bone, all seven maxillae are ornamented laterally with tubercles that can be isolated or coalesce into anastomosing bony ridges at the periphery of the bone. The presence of this dermic ornamentation in the maxilla is a characteristic trait of *Pelobates* (Bailon, 1999). The maxilla is elongate, and its ventral edge, the cresta dentalis, bears pleurodont teeth. In medial view, the processus palatinus, incomplete in all the available

Fig. 2. Photographs of fossil anuran bones from the Early Pleistocene site of Pirro Nord 13 (Apricena, southern Italy). **A**–**G**, *Pelobates syriacus* (Pelobatidae): **A**, left maxilla (MGPT-PU 150706), in labial (**A1**) and lingual (**A2**) views; **B**, sphenethmoid (MGPT-PU 150612), in dorsal (**B1**), anterior (**B2**) and ventral (**B3**) views; **C**, trunk vertebra (MGPT-PU 150932), in dorsal (**C1**), ventral (**B2**), anterior (**C3**), and posterior (**C4**) views; **D**, sacrum with the anteriormost end of the urostyle (MGPT-PU 150704), in ventral view; **E**, left scapula (MGPT-PU 150735), in dorsal (**E1**) and ventral (**E2**) views; **F**, right humerus (MGPT-PU 150665), in ventral view; **G**, right ilium (MGPT-PU 150664), in lateral (**G1**) and medial (**G2**) views. **H**–**L**, *Bufotes viridis* gr. (Bufonidae): **H**, atlas (MGPT-PU 150878), in anterior (**H1**), posterior (**H2**) and right lateral (H3) views; **I**, sacrum (MGPT-PU 142860), in dorsal (**I1**) and ventral (**I2**) views; **J**, left scapula (MGPT-PU 150689), in dorsal view; **K**, left humerus of male (MGPT-PU 150691), in ventral (**K1**) and medial (**K2**) views; **L**, left humerus of female (MGPT-PU 150702), in ventral view; **M**, right ilium (MGPT-PU 150928), in lateral view. **N**–**P**, *Bufo* gr. *B. bufo* (Bufonidae): **N**, right scapula (MGPT-PU 150893), in dorsal view; **O**, left humerus of female (MGPT-PU 150734), in ventral view; **P**, left ilium (MGPT-PU 150491), in lateral view. **Q**–**S**, *Pelophylax* cf. *esculentus/ridibundus* (Ranidae): **Q**, left ilium (MGPT-PU 150618), in lateral (**Q1**) and posterior (**Q2**) views; **R**, urostyle (MGPT-PU 150701), in dorsal (**R1**) and anterior (**R2**) views; **S**, coracoid (MGPT-PU 150620), in ventral view. Images at different magnifications (see corresponding 2 mm scale bars).

fossils, is rather thick and directed anteromedially. A well delimited and concave fossa maxillaris is present, between the proximal part of the processus palatinus and the anterior part of the lamina horizontalis. The lamina horizontalis is straight and relatively narrow close to the premaxillary-maxillary suture and increases in width posteriorly; likewise, its margins gradually increase in thickness.

We recovered two sphenethmoids in PN13 (Fig. 2B). The sphenethmoids are elongate and strongly flattened dorsoventrally, and they bear prominent anterior and lateral processes. These traits are characteristics of the genus *Pelobates* (Bailon, 1999). In anterior view, the sella amplificans folds are clearly visible on the floor (solum nasi) of each anterior alveolus (= capsula ethmoidalis or antrum olfactorium). Although incomplete in both specimens, the processus praenasalis medius seem to have been rather long and wide, at least posteriorly.

Variably developed laminae supraorbitalis are visible on each side of the bone, on the posterior part of the lateral processes. The fenestra frontoparietalis is deep and posteriorly wide, and its anterior margin is rounded. The dorsal surface of the element bears a small, triangular patch covered with irregular dorsal ornament. This triangular surface represents the area not covered by the nasals anteriorly and the frontoparietals posteriorly. In ventral view, the lateral processes project outwards from the main body of the bone, are oriented slightly anterolaterally, and show a V-shaped arrangement of anteriorly and posteriorly bifurcating ridges that demarcate the contact surface for the processus palatinus of the maxilla. A foramen (canalis ophthalmicus medialis) perforates the base of the lateral processes. On the posteromedial area of the ventral surface, it presents a long and narrow scar, sometimes with some ridges on its anterior part. Just forward of that elongate scar is a circular and shallow scar. In anterior view, the bone is about four times wider than high, and the folds (sella amplificans) reach more than half the height of the capsulae ethmoidalis. Located on each side of the septum nasi, the canalis ophthalmicus medialis are relatively well developed and higher than wide. The canalis ophthalmicus lateralis are rather wide and located slightly medially within the capsulae ethmoidalis.

The vertebrae (Fig. 2C) are consistently procoelous, with an anterior cotyle and a posterior condyle. In anterior view, the anterior cotyle is deep and approximately circular in the posterior vertebrae. The posterior condyle is robust and round, and it is clearly delimited from the centrum by a step. The neural arch is anteroposteriorly elongated and dorsoventrally flattened, and it shows a moderate interzygaphyseal constriction in dorsal view. The anterior edge is variously concave, whereas the posterior edge bears a pointed median process than on some vertebrae surpasses the posterior edge of the prezygapophyses. The presence of a circular cotyle and condyle, an elongated neural arch, and a developed posterior pointed median process is a characteristic trait of the dorsal vertebrae of *Pelobates*, which allows its differentiation from other anurans (Bailon, 1999).

The sacra are solidly fused with the urostyle, although in the two recovered specimens the urostyle is posteriorly incomplete (Fig. 2D). They are procoelous and bear transverse processes that are broadly expanded anteroposteriorly and have straight lateral margins. This fusion of the sacra with the urostyle together with the broad anteroposterior expansion of the transverse processes are distinguishing features of *Pelobates syriacus* and *Pelobates fuscus* (Bailon, 1999; Blain et al., 2016b). In *Pelobates cultripes*, the urostyle is not fused with the sacra (Bailon, 1999). The sacra bear a low, slender and pointed neural spine that extends posteriorly for a short distance above the dorsal surface of the urostyle. The prezygapophyses are nearly circular. The preserved portion of the urostyle lacks a dorsal crest but bears lateral laminar expansions that are fused anteriorly with the transverse processes.

The scapulae (Fig. 2E) are relatively robust and clearly higher than wide. The pars glenoidalis is distinct from the main corpus of the bone, and in the dorsal view is partially hidden by the pars acromialis. The surface of articulation with the humerus extends across the pars glenoidalis and onto the posterior margin of the pars acromialis, distinguishing trait of the genus *Pelobates* (Bailon, 1999). The anterior margin of the scapula is slightly concave, and it bears a poorly developed and short crista anterior.

We recovered five humeri of *Pelobates syriacus* in PN13. In the most complete humerus (Fig. 2F), the preserved portion of the diaphysis is robust and slightly curved, and bears a main crista ventralis and medially a smaller crista paraventralis. The condyle is spherical, well ossified and slightly displaced laterally relative to the diaphysis main axis. The fossa cubitalis ventralis is relatively large, deep and open radially. The epicondylus ulnaris is not fully preserved in the recovered humeri. The epicondylus radialis is small, and it is topped by a small crista lateralis. A long and narrow crista medialis is present along the medial margin. The presence of a curved diaphysis, a crista paraventralis, and a radially opened fossa cubitalis ventralis is a diagnostic feature of the genus *Pelobates* (Bailon, 1999).

The ilia (Fig. 2G) are characterised by the absence of crista dorsalis, tuber superior and preacetabular and supracetabular fossae, and by the presence of a wide and strongly striated interiliac articulation surface and a short pars ascendens with a straight dorsal edge. These traits are characteristic of the genus *Pelobates* (Bailon, 1999; Blain et al., 2016b). The acetabulum is well developed and semicircular in lateral outline. The pars descendens, although not fully preserved in the recovered specimens, is relatively wide.

Family Bufonidae Gray, 1825.

We attributed forty-seven elements, mainly fragmentary bones or bones with low diagnostic value preventing a more precise attribution at the family level, belonging to either genera *Bufotes* or *Bufo* (2 vertebrae, 5 coracoids, 1 humerus, 23 radioulnae, and 16 tibiofibulae).

Genus *Bufotes* Rafinesque, 1815.

Bufotes viridis (Laurenti, 1768) – Green Toad.

Bufotes viridis gr.

(Fig. 2H–M)

Material: 1 atlas, 13 vertebrae, 7 sacra, 6 urostyles, 5 scapulae, 53 humeri, 39 ilia, and 7 femora.

Description: The green toad is by far the most represented anuran in PN13 (63.9 % in terms of MNE, and 63.6 % in terms of MNI). We have recovered only one atlas of *Bufotes viridis* gr. (Fig. 2H). The bone is procoelous, and it bears a robust and dorsoventrally flattened condyle. The vertebral centrum is well individualised. The neural arch is short, with robust lateral walls, and the neural crest is thick posteriorly. In lateral view, it presents a small bony expansion (= subzygapophyseal spine) below the postzygapophyses. The subzygapophyseal spine is present in the *Bu. viridis* gr., whereas in other bufonids such as *Epidalea calamita* and the *Bufo* gr. *B. bufo*, this bony feature is only weakly developed (Bailon, 1999).

The vertebrae are procoelous, with a broad condyle. They have a developed vertebral centrum with short and robust lateral walls, and a short neural arch, features characteristic of the family Bufonidae (Bailon, 1999).

The sacra (Fig. 2I) have an anterior cotyle and two posterior condyles. They are characterised by the presence of anteroposteriorly wide sacral apophyses and a W-shaped neurapophysis. Adeep, laterally open notch is presentat the base of each sacral apophyses, a characteristic trait of *Bu. viridis* gr. (Bailon, 1999).

We attributed six urostyles to *Bu. viridis* gr. All of them present a moderately developed crista dorsalis and are devoid of transverse apophyses (= processus transversus) or horizontal blade (= lamina horizontalis). On the anterior view, they exhibit two cotyles (= fossa condyloidea) well individualised between them and slightly flattened dorso-ventrally.

The recovered scapulae are well preserved (Fig. 2J). They are robust, short and wide. The pars glenoidalis is distinct from the main corpus of the bone and clearly visible in dorsal view. A small supraglenoidal fossa is frequently present, in contrast to *Bufo* gr. *B. bufo*, where this feature is absent (Bailon, 1999). The pars acromialis has anterior and ventral edges more or less rounded; the anterior margin of the scapula is slightly concave, and it bears a crista anterior weakly developed.

The humerus is the most represented bone of *Bu. viridis* gr. recovered in PN13, documenting both female (Fig. 2K) and male (Fig. 2L) individuals. The diaphysis is rectilinear in males and slightly curved in females, in both cases a crista ventralis is present. The male humeri display a dorsally curved and long crista medialis, whereas in *Bufo* gr. *B. bufo*, the crista is nearly flat and restricted to the distal part of the epiphysis (Bailon, 1999; Delfino and Bailon, 2000). This crista is usually absent in females (Bailon, 1999). The condyle is spherical, weakly ossified and displaced on the radial side in comparison to the diaphysis main axis. The fossa cubitalis ventralis is relatively large, deep and open radially. The epicondyles are moderately developed.

The ilia (Fig. 2M) are characterised by an ilial shaft devoid of crista

dorsalis, and by the presence of a high tuber superior that usually expresses a secondary anterior tubercle. A well-developed and deep fossa preacetabularis is present, a diagnostic trait of *Bu. viridis* gr. (Bailon, 1999; Delfino and Bailon, 2000).

The femora, although they do not preserve the epiphyses, are relatively robust and display a high sharp and partially divided crista femoris. In *Bufo* gr. *B. bufo*, the crista femoris is divided and forms a triangular shape, while in *Bu. viridis* gr., a partial or incipient division is often present (Bailon, 1999).

Genus *Bufo* Garsault, 1764

Bufo bufo (Linnaeus, 1758) – the common toad or *Bufo spinosus* Daudin, 1803 – the spiny toad.

Bufo gr. *B. bufo*.

(Fig. 2N–P)

Material: 3 vertebrae, 1 scapula, 4 humeri, 1 radioulna, 3 ilia, and 5 tibiofibulae.

Description: One incomplete right scapula (Fig. 2N) is attributable to *Bufo* gr. *B. bufo*. The preserved part of the bone is large (11 mm long and 9 mm wide) and relatively robust. It bears a robust, detached pars glenoidalis that is clearly visible in dorsal view. Besides the size and general robustness of this fossil, the attribution to *Bufo* gr. *B. bufo* is supported by the lack of supraglenoidal fossa on the base of the pars glenoidalis, a characteristic trait of this species (Bailon, 1999).

The recovered humeri document female (Fig. 2O) and male (not figured) individuals. The humeri are robust and, in ventral view, show a diaphysis that is rectilinear in males and slightly curved in females. Their condyles, weakly ossified, are displaced on the radial side in comparison with the diaphysis main axis.

The ilia (Fig. 2P) are devoid of crista dorsalis and present a low and rounded unilobated tuber superior like in *Bufo* gr. *B. bufo*, whereas in *Bu. viridis* gr. the tuber superior is usually bilobated (Bailon, 1999).

In the case of some complete but lesser diagnostical elements (as vertebrae, radioulna, and tibiofibulae), we made the specific attribution between these elements using size and robustness as a criterion.

The former species (*Bufo bufo* s.l.) has been divided into two distinct species based mainly on genetic and external characters (Arntzen et al., 2013): *Bufo bufo* sensu stricto (most of Europe and the western part of North Asia) and *Bufo spinosus* (Iberian Peninsula, the south-western half of France following a suture line between the two species from Normandy to Franche-Comté Regions, and North-Africa). No osteological characters have been described that would permit the differentiation between the two species. In conclusion, the attribution of our fossils is conservatively done at the level of the group *B. bufo* and *B. spinosus*.

Family Ranidae Batsch, 1796.

Genus *Pelophylax* Fitzinger, 1843.

Pelophylax kl. *esculentus* (Linnaeus, 1758) – the edible frog/*Pelophylax ridibundus* (Pallas, 1771) – the marsh frog.

Pelophylax cf. *esculentus/ridibundus*.

(Fig. 2Q–S)

Material: 3 vertebrae, 2 urostyles, 1 scapula, 3 coracoids, 4 humeri, 2 radioulnae, 9 ilia, and 1 femur.

Description: Attribution to waterfrogs (genus *Pelophylax*) is based on scapula and ilia, mainly. The other elements, presenting similar morphology than described for ranids, have been reported to *Pelophylax* cf. *esculentus/ridibundus* by association with the diagnostic elements recovered in PN13.

The scapula is higher than wide. In dorsal view, the pars glenoidalis is totally hidden by the pars acromialis, like in ranids. In ventral view, it presents a short internal crest on the ventral surface of the pars glenoidalis, a characteristic trait of *Pelophylax*, while in *Rana* this crest is longer and is also extended to the lamina ossea (Bailon, 1999).

The ilia (Fig. 2Q) are the most numerous elements attributed to *Pelophylax* cf. *esculentus/ridibundus*. They are characterised by the presence of a high and vertical ilial crest (= crista dorsalis) on the shaft, a short ischial process (= pars ascendens). The presence of a high crista dorsalis is characteristic of *Pelophylax*, whereas in genus *Rana* this crest is generally much lower (Bailon, 1999). They exhibit a well-developed laterally flattened tuber superior, as is characteristic in *Pelophylax esculentus/ridibundus*, whereas in *Pelophylax lessonae*, the tuber is laterally prominent and steeper (Böhme and Günther, 1979; Blain et al., 2015).

Three amphicoelous vertebrae correspond to the 8th vertebra. This vertebra is characteristic of Ranidae (Bailon, 1999).

The urostyles (Fig. 2R) present two circular cotyles anteriorly (= fossa condyloidea) and lack any transverse processes. The neural arch is relatively narrow. Although partially broken in both cases, the neural crest (= crista dorsalis) is long and high.

The coracoids (Fig. 2S) present a thick distal end (= pars epicoracoidales) and a flat and wide proximal one (= pars glenoidalis), although the pars glenoidalis is not fully complete in our fossils. The anterior margin is strongly concave.

We recovered four incomplete female humeri have in PN13. These elements present a straight diaphysis with the condyle located on the main axis of the diaphysis. The crista medialis is absent.

The radioulnae present a less robust neck, and an olecranon process relatively more ossified than in the bufonids.

We have attributed a quite complete femur to *Pelophylax* cf. *esculentus/ridibundus*. It is long and thin and does not have a femoral crest (= crista femoris), like in Ranidae (Bailon, 1999).

Class Reptilia Laurenti, 1768.

Order Squamata Oppel, 1811.

In the context of squamate remains, we have categorised 261 elements within a higher rank category. Of these, 7 have been attributed to Lacertilia indet., encompassing one fragmented maxilla, one undetermined tooth bearing bone, three fragmented vertebrae, and two incomplete femora.

We have attributed the remaining 254 elements to Serpentes indet., encompassing some 213 vertebrae (mainly cervical and caudal vertebrae, and fragmentary undeterminable vertebrae), 3 fragmentary dentaries, and 38 ribs.

Family Lacertidae Batsch, 1788

The taxonomic allocation of lacertid remains is based on several cranial elements (Villa and Delfino, 2019) other than the teeth bearing bones that were traditionally used. The dentition is distinguished by the presence of pleurodont teeth, typically bicuspid, and approximately cylindrical in shape. We have not considered the number of teeth and the number of foramina on the lateral wall of the dentaries and maxillae taxonomic allocation because they are related to the age and size of the individual (Roček, 1980; Mateo, 1988; Mateo and López-Jurado, 1997). According to their relative size, the lacertid remains can be separated into two different categories. The first category (Lacertidae indet., large-sized) refers to medium and large-sized lacertids, including the species *Lacerta bilineata, Lacerta viridis* and *Timon lepidus*. The second category (Lacertidae indet., small-sized) is primarily attributable to the extant species *Podarcis sicula* and *Podarcis muralis*, though consideration must be given to certain Balkan small-sized lacertid genera (e.g. *Dinolacerta*, *Hellenolacerta*, or *Algyroides*). However, in the absence of more extensive morphological analyses of these later taxa, the small-sized lacertid remains recovered in PN13 are carefully referred to cf. *Podarcis* sp.

cf. *Podarcis* sp. (Fig. 3A–C)

Material: 2 maxillae, 67 dentaries, 8 undetermined tooth-bearing bones, 13 trunk vertebrae, 2 caudal vertebrae, 4 hemipelves, and 2 femora.

We have identified two small-sized maxillae at the site. Despite the incompleteness of both bones, the preserved teeth are bicuspid and are projected beyond the crest for half their total length in both cases. In lateral view, the surface of the bones does not display any ornamentation, and labial foramina are present.

The dentaries are by far the most numerous small-sized lacertid element recovered. They are elongated and gracile, with a total preserved length between 6 and 7 mm. In most cases, the posterior

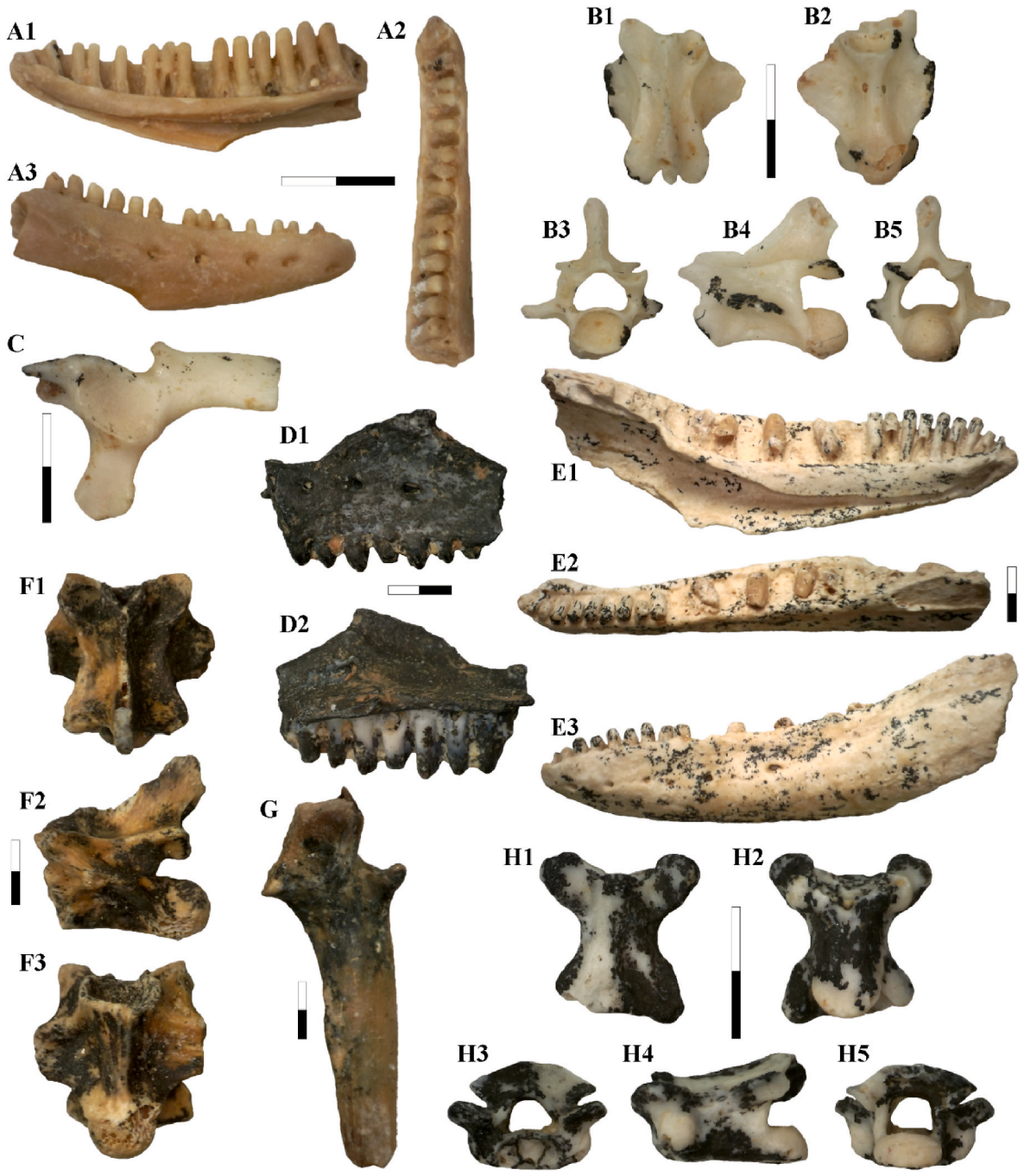

Fig. 3. Photographs of fossil lizard and amphisbaenian bones from the Early Pleistocene site of Pirro Nord 13 (Apricena, southern Italy). **A**–**C**, cf. *Podarcis* sp. (Lacertidae): **A**, right dentary (MGPT-PU 150679), in lateral (**A1**), dorsal (**A2**), and medial (**A3**) views; **B**, caudal vertebra (MGPT-PU 150959), in dorsal (**B1**), ventral (**B2**), anterior (**B3**), left lateral (**B4**), and posterior (**B5**) views; **C**, left hemipelvis (MGPT-PU 150611), in lateral view. **D**–**G**, *Lacerta* s.l. (Lacertidae): **D**, left maxilla (MGPT-PU 150869), in lateral (**D1**) and medial (**D2**) views; **E**, left dentary (MGPT-PU 150679), in lateral (**E1**), dorsal (**E2**), and medial (**E3**) views; **F**, caudal vertebra (MGPT-PU 15678), in dorsal (**F1**), left lateral (**F2**), and ventral (**F3**) views; **G**, left hemipelvis (MGPT-PU 150611), in lateral view. **H**, *Blanus* sp. (Blanidae): trunk vertebra (MGPT-PU 15708), in dorsal (**H1**), ventral (**H2**), anterior (**H3**), left lateral (**H4**), and posterior (**H5**) views. Images at different magnifications (see corresponding 2 mm scale bars).

projections are not preserved. One of the most complete specimens (Fig. 3A) exhibits 19 tooth positions, of which 13 teeth are preserved. All of them are bicuspid and project a little bit less than half of their total length beyond the dental crest (= crista dentalis). In medial view, the Meckelian canal is open along its entire length and the subdental shelf is rather thick anteriorly. In lateral view, the surface is smooth and presents five mental foramina. The length of the dental shelf matches the size of the extant adults small-sized lacertids as *Podarcis* species (Barahona and Barbadillo, 1997). The projection of the teeth beyond the dental crest, together with the slender aspect of the teeth, is consistent with a representative of the genus *Podarcis* (see Blain et al., 2007).

The small-size (centrum lengths are comprised between 2 and 3 mm) procoelous trunk and caudal vertebrae (Fig. 3B), two femora, and four hemipelves (Fig. 3C) have a morphology and estimated size that appear to be concordant with the extant *Podarcis*.

Lacerta s.l. (Fig. 3D–G)

Material: 1 maxilla, 5 dentaries, 7 trunk vertebrae, 2 caudal vertebrae, and 1 hemipelvis.

The large-sized lacertid is represented by a small number of remains. All the recovered elements are incomplete, as is the case for the maxilla (Fig. 3D) and dentaries (Fig. 3E). However, the teeth are isodont, cylindrical and mono-, or bicuspid, and, on the dentaries, the Meckelian canal is wide open. Preserved teeth on the maxilla are mainly bicuspid and do not project more than one third of their total length beyond the dental crest (= crista dentalis), which, according to Barahona Quintana (1996) and Barahona and Barbadillo (1997), agrees with the extant species of genus *Timon* and *Lacerta bilineata*. The dentaries are relatively robust, with mainly bicuspid teeth that project poorly (less than one third of their total length) beyond the dental crest. In medial view, the subdental shelf is thick and robust.

The remaining elements, i.e. the trunk and caudal vertebrae (Fig. 3F) and the hemipelves (Fig. 3G), are characteristic of the family and only their relatively large size permits to include them into this category.

Family Blanidae Kearney, 2003.

Genus *Blanus* Wagler, 1830.

Blanus sp. – a worm lizard.

(Fig. 3H)

Material: 27 trunk vertebrae.

Description: All the recovered trunk vertebrae are small (centrum length < 3 mm) and procoelous, with an anterior cotyle and a posterior condyle, both are dorsoventrally flattened (Fig. 3H). In ventral view, the centrum is generally longer than wide and possesses a flat ventral surface with parallel or slightly convex margins. The prezygapophyses and postzygapophyses are well-developed and inclined upward. The neural arch is dorsoventrally flattened and has a concave posterior end and a well-marked interzygapophyseal constriction. The neural spine is reduced. In lateral view the synapophyses are globular and more or less circular. The identification at genus rank of isolated amphisbaenian vertebrae is not possible (Villa et al., 2019) but the morphology of the vertebrae from PN13 here reported is fully congruent with that of the vertebrae associated to diagnostic cranial elements described from other approximately coeval fissures of the Pirro Nord complex (Delfino and Bailon, 2000).

Family Natricidae Bonaparte, 1840

Genus *Natrix* Laurenti, 1768

Natrix natrix (Linnaeus, 1758) – the grass snake.

Natrix gr. *N. natrix*.

(Fig. 4)

Material: 92 trunk vertebrae.

Description: Trunk vertebrae have a well-developed hypapophysis and, in posterior view, the neural arch is convex, as in genus *Natrix*. The condyle and cotyle are relatively small and circular. The attribution to a grass snake is mainly based on the morphology of the centrum, with a flat ventral surface and with well-marked lateral margins, whereas in *Natrix maura* these lateral margins are more or less diffuse and the centrum ventral surface is slightly convex laterally (Szyndlar, 1984). The hypapophysis and parapophyseal processes, although not fully preserved on the largest vertebrae (as the one figured, Fig. 4), are robust and with a generally obtuse tip like in grass snakes, whereas in *N. maura* and *Natrix tesselata* these processes are slender and with a pointed tip (Szyndlar, 1984).

Family Colubridae Oppel, 1811.

Colubridae indet.

Material: 183 trunk vertebrae.

We have assigned several trunk vertebrae without hypapophysis to family level only, as they are incomplete and/or exhibit inconsistent features.

Genus *Coronella* Laurenti, 1768.

Coronella austriaca Laurenti, 1768– the smooth snake.

Coronella cf. *C. austriaca*.

(Fig. 5A)

Material: 28 trunk vertebrae.

Description: These vertebrae are small, with a centrum length always shorter than 5 mm and, in posterior view, with a neural arch strongly dorsoventrally flattened. The ventral surface of the centrum does not bear any hypapophysis and the haemal keel is smooth, rather well defined, and its posterior end is slightly spatulated. The prezygapophyseal processes are usually short, wide at their basis and with

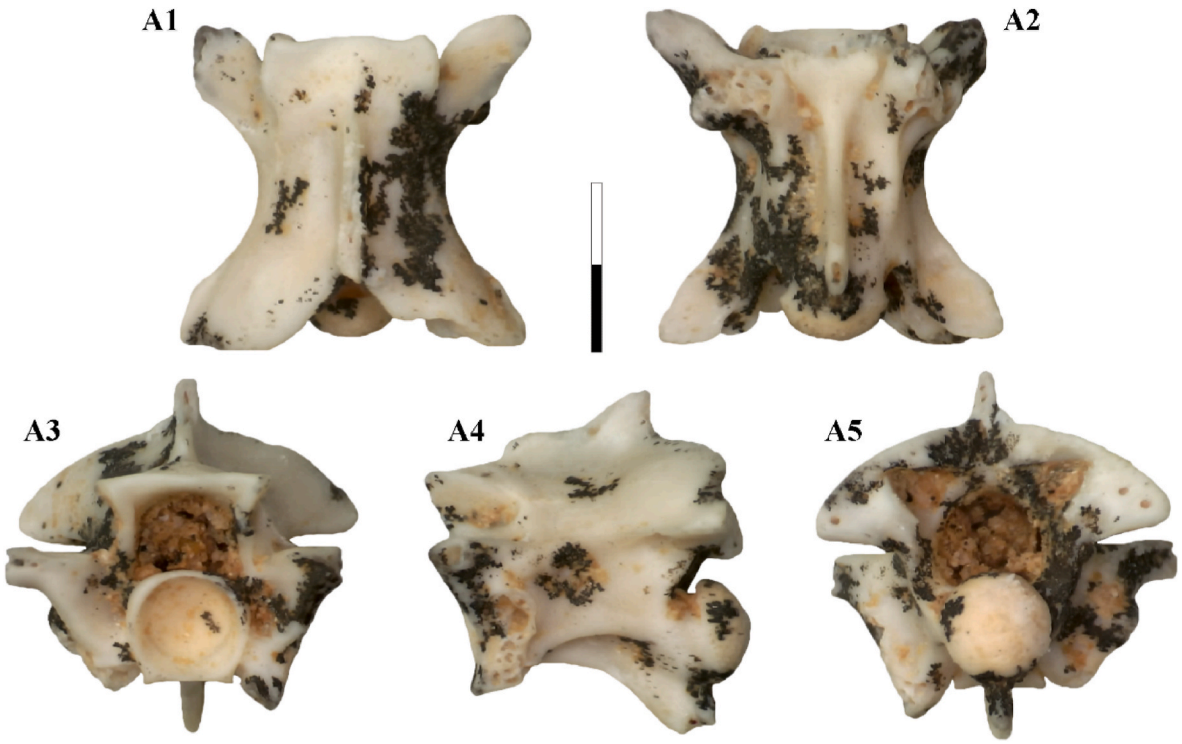

Fig. 4. Photographs of fossil snakes (Natricidae) bones from the Early Pleistocene site of Pirro Nord 13 (Apricena, southern Italy). **A**, *Natrix* gr. *N. natrix*: trunk vertebra (MGPT-PU 150939), in dorsal (**A1**), ventral (**A2**), anterior (**A3**), left lateral (**A4**), and posterior (**A5**) views. Scale = 2 mm.

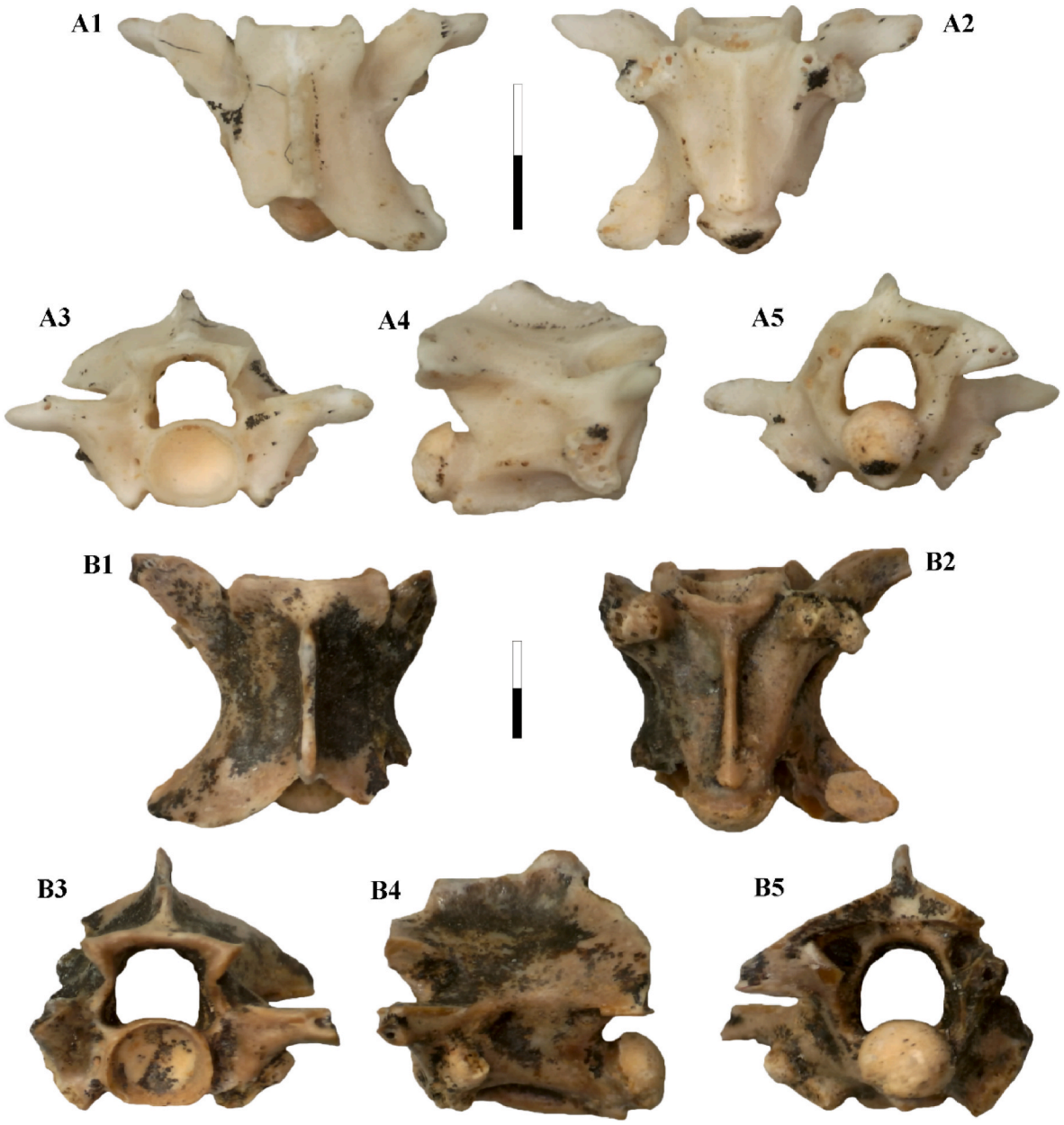

Fig. 5. Photographs of fossil snakes (Colubridae) bones from the Early Pleistocene site of Pirro Nord 13 (Apricena, southern Italy). **A**, *Coronella* cf. *C. austriaca*: trunk vertebra (MGPT-PU 150914), in dorsal (**A1**), ventral (**A2**), anterior (**A3**), right lateral (**A4**), and posterior (**A5**) views. **B**, *Zamenis* gr. *Z. longissimus*: trunk vertebra (MGPT-PU 150870), in dorsal (**B1**), ventral (**B2**), anterior (**B3**), right lateral (**B4**), and posterior (**B5**) views. Images at different magnifications (see corresponding 2 mm scale bars).

an obtuse and rounded tip, like in *C. austriaca*, while in *Coronella girondica* these are narrower at the basis, somewhat longer, and usually end with a pointed tip (Szyndlar, 1984; Bailon, 1991). Another diagnostic character is the size of the parapophyses in relation to the diapophyses, which are longer in *C. austriaca* when compared to *C. girondica* (Szyndlar, 1984; Bailon, 1991). Despite the presence of these morphological characters in the recovered vertebrae the attribution to *C. austriaca* must be considered tentative, given the high degree of variability exhibited by these characters (see Delfino and Bailon, 2000).

Genus *Zamenis* Wagler, 1830.

Zamenis longissimus (Laurenti, 1768) – the Aesculapian snake or *Zamenis lineatus* (Camerano, 1891) – the Italian Aesculapian snake.

Zamenis gr. *Z. longissimus*.

(Fig. 5B)

Material: 186 trunk vertebrae.

Description: The trunk vertebrae of *Zamenis* gr. *Z. longissimus* documented in PN13 are of a medium and large size, with a mean centrum length of 6 mm. These vertebrae are distinguished by a high and rounded haemal keel that is spatulate at the posterior end, like in *Zamenis lineatus* and *Zamenis longissimus*, while in *Zamenis situla* the haemal keel is non pronounced (Szyndlar, 1984). The prezygapophyseal processes are relatively short and show a rounded tip, characteristic of *Zamenis* gr. *Z. longissimus* (although they are slender and pointed in the smallest specimens) (Szyndlar, 1984). In anterior view, the zygosphene is generally straight anteriorly, as it is usual in large specimens (Szyndlar, 1991). The species *Z. lineatus* and *Z. longissimus* exhibit a similar morphology for the trunk vertebrae, and consequently, in the absence of diagnostic characteristics, these PN13 remains are referred to *Zamenis* gr. *Z. longissimus*.

3.2. Palaeoclimatic reconstruction

The obtained palaeoclimatic results are valid for the SUs A, B, and C, on the basis that the same species of amphibians and reptiles have been documented in all three units (Table 1). It is also reasonable to consider them valid for SU D, despite the sparse sample available, given that the species *Pelobates syriacus* has been documented there too, based on the samples hosted in the University of Ferrara, Italy (see Blain et al., 2016b).

Application of the MER method with the UDA-ODA discrimination technique to the PN13 palaeoherpetofaunal assemblage has resulted in a common overlapping area of 12,923 km^2. These areas are situated between the Balkan Peninsula and the Black Sea, encompassing the present-day countries of Bulgaria, North Macedonia and in a reduced region of Northern Greece (Fig. 6).

The estimated Mean Annual Temperature (MAT) is 11.3 ± 1.7 °C and the Mean Annual Precipitation (MAP) is 599 ± 66 mm (Table 3). To achieve a better visualization of the monthly evolution of temperature and precipitation, we have produced climatograms, applying the scale P = 2 x T to directly evaluate the Gaussen index. The climatic interpretation is summarised in Table S4. The reconstructed climate can be characterised as cold and continental (i.e., with a very high atmospheric temperature range), with warm-temperate summer and cold winter. Rainfalls are low and with a regular distribution during the year, occurring primarily during winter and spring. The aridity indexes suggested a humid (or semi-humid according to De Martonne's index) continental Mediterranean climate with two dry months in July and August (Fig. 7A, Table 4).

Despite the exclusion of *Blanus* sp. from the MER analysis, our palaeoclimatic inferences are in alignment with its known ecology. In particular, the climatic spectrum associated with the extant representatives of the genus *Blanus* (i.e., *Bl. cinereus* complex and *Bl. strauchi* complex) falls within the range of conditions reflected in our results.

Comparison between our palaeoclimatic inferences and the current climatic data for the PN13 site location (1970–2000; Fig. 7A–Table 3) showed the estimated MAT to be lower than at present (ΔMAT = −4.4 °C), with colder summers (ΔMTW = −3.4 °C) and much colder winters (ΔMTC = −6.8 °C). The total amount of rainfall was slightly higher than at present (ΔMAP = +45 mm), with a more regular distribution throughout the year. At present, the rainfall regime shows greater seasonality, with higher levels of precipitation occurring during the winter months. The aridity indexes suggested similar climatic interpretations (Table 4), in both cases pointing to semi-humid conditions. However, if we look at the index's values, for the Pleistocene they were closer to those attributable to humid conditions, while for the present they were closer to those attributable to semi-arid conditions (see Table S4). This divergence was further substantiated by the Dantin-Revenga aridity index.

3.3. Palaeoenvironmental reconstruction

Application of the Habitat Weighting method suggested a potential greater representation of open environments over woodlands (Fig. 7B). Open environments were primarily composed of open-dry habitats (29.59 %) and, to a lesser extent, of open-humid habitats (15.54 %) and rocky-stony landscapes (13.92 %). The presence of woodland environments was also inferred, including medium scrublands to forest formation (19.12 %), with aquatic and peri-aquatic areas (21.82 %), such as rivers or ponds with riverside vegetation.

The analysis of the different SUs separately showed more or less the same representations and proportions of habitats (Fig. 7B), with the exception of the SU C, where the open-humid habitats were somewhat more represented than in the other SUs.

3.4. Fossil assemblages and species interrelationship

For the Pirro Nord fissures that have been used in the data matrix, the most representative taxa were cf. *Podarcis* sp. (present in 20 assemblages, 80 % of the total), *Lacerta* s.l. (18 assemblages, 72 %) and *Testudo hermanni* (16 assemblages, 64 %), and to a lesser extent *Pelophylax* sp. (9 assemblages, 36 %) and *Emys orbicularis* (8 assemblages, 32 %). Together, these species form a typical association in current warm

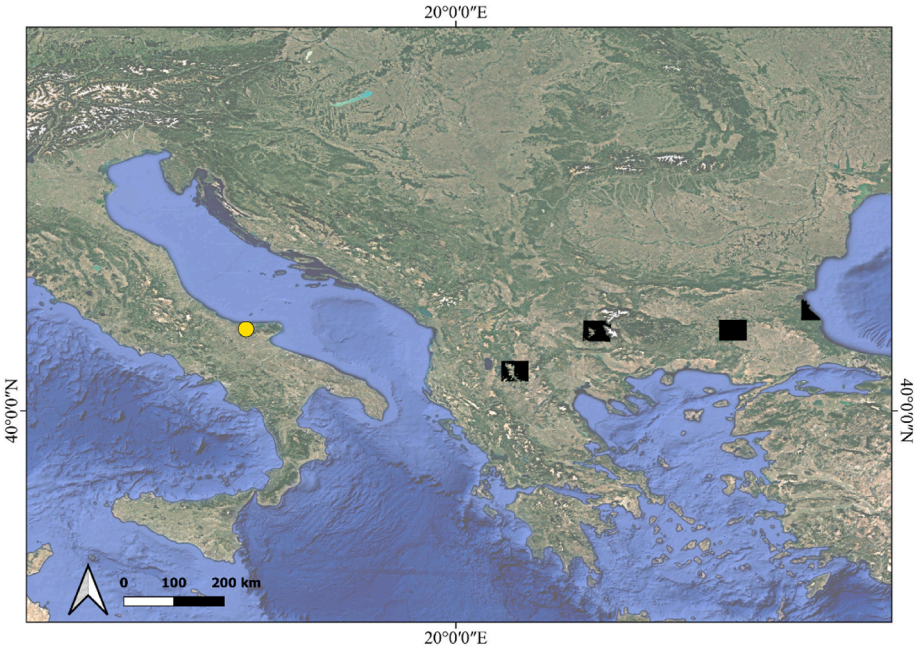

Fig. 6. Map illustrating the final overlapping areas of the current distribution of the amphibians and reptiles of the Early Pleistocene site of Pirro Nord 13 (Apricena, southern Italy), resulting from the MER (Mutual Ecogeographic Range) method and the UDA-ODA (Uncertain Distribution Area-Occupied Distribution Area) discrimination technique. The black areas on the map correspond to the 50 × 50 km species distribution squares from Sillero et al. (2014) after the removal of those areas exceeding the upper elevation boundary where all the species could potentially coincide (1200 m). The yellow dot indicates the location of the PN13 site. The geographic coordinates are represented in the WGS 84 spatial reference system. Abbreviations: km = kilometres.

Table 3
Climatic values for the Early Pleistocene site of Pirro Nord 13 (Apricena, southern Italy), calculated by the MER (Mutual Ecogeographic Range) method and the UDA-ODA (Uncertain Distribution Area-Occupied Distribution Area) discrimination technique, and values of the PN13 site location nowadays (1970–2000; Fick and Hijmans, 2017). Temperature in °C and precipitation in mm. Abbreviations: MAP = mean annual precipitation, MAT = mean annual temperature, MAX = maximum, MIN = minimum, SD = standard deviation.

	Temperature (°C)												
	MAT	J	F	M	A	M	J	J	A	S	O	N	D
Pirro Nord 13													
MEAN	11.3	0.8	2.6	5.8	10.3	15	19	21.2	20.9	17.5	12.5	7.1	2.7
SD	1.7	1.5	1.4	1.4	1.7	1.7	1.9	1.9	1.9	1.7	1.7	1.9	1.7
MIN	6.5	−2.9	−1.4	1.3	5	9.7	13.2	15.6	15.4	12.2	7.7	2.9	−1
MAX	14.4	3.7	5.4	9.1	13.9	18.7	22.6	25	24.5	21.2	15.8	10.4	6.3
Nowadays (1970–2000)													
MEAN	15.7	7.6	8.3	10.2	13.2	17.6	21.7	24.5	24.6	21.4	17	12.5	9.2
SD	0.2	0.2	0.2	0.2	0.2	0.2	0.2	0.1	0.1	0.2	0.2	0.2	0.2
MIN	15.4	7.2	7.9	9.8	12.9	17.3	21.4	24.2	24.4	21.1	16.6	12.2	8.8
MAX	15.9	7.9	8.6	11	13.5	17.8	21.9	24.7	24.9	21.7	17.3	12.9	9.6
Δ													
MEAN	−4.4	−6.8	−5.7	−4.4	−2.9	−2.6	−2.7	−3.3	−3.7	−3.9	−4.5	−5.4	−6.5
	Precipitation (mm)												
	MAP	J	F	M	A	M	J	J	A	S	O	N	D
Pirro Nord 13													
MEAN	599	53	48	48	49	59	49	37	31	38	52	71	64
SD	66	9	7.1	6.6	5.8	7.7	5.1	4.3	5.2	6	12.3	10.7	9,9
MIN	470	33	34	36	28	42	40	27	21	26	37	54	46
MAX	846	82	69	74	73	79	67	47	45	52	89	107	90
Nowadays (1970–2000)													
MEAN	555	55	42	43	44	37	32	28	32	51	60	63	68
SD	5.8	0.9	0.6	0.6	1	0.5	0.4	0.5	0.5	0.3	0.6	0.8	0.8
MIN	544	53	41	42	42	36	32	27	32	50	59	62	67
MAX	565	57	43	44	45	37	33	29	33	51	61	65	70
Δ													
MEAN	45	−2	6	5	6	23	17	9	−1	−13	−8	8	−4

Italian environments, specially associated with Mediterranean coastal areas and large alluvial plains (Blain et al., 2019). The other represented taxa were *Bufo* gr. *B. bufo* (7 assemblages, 28 %), *Natrix* gr. *N. natrix* (7 assemblages, 28 %), *Hierophis viridiflavus* (5 assemblages, 20 %), *Zamenis* gr. *Z. longissimus* (5 assemblages, 20 %), *Bufotes viridis* gr. (3 assemblages, 12 %), *Mauremys* sp. (3 assemblages, 12 %), *Hyla* gr. *H. arborea* (2 assemblages, 8 %), *Coronella* cf. *C. austriaca* (2 assemblages, 8 %), *Pelobates syriacus* (1 assemblage, 4 %) and *Blanus* sp. (1 assemblage, 4 %).

The resulting hierarchical cluster by species (Fig. S1A), which had a high value of cophenetic correlation coefficient (*cophen. corr.* = 0.8922), distinguished three major groups: the first group was formed by the taxa *Pelophylax* sp., *E. orbicularis*, *T. hermanni*, cf. *Podarcis* sp. and *Lacerta* s.l., an association of heliophile herpetofauna that were the predominant taxa in the fossil record. The second group was composed by the species *Bufo* gr. *B. bufo*, *H. viridiflavus*, *Zamenis* gr. *Z. longissimus* and *Natrix* gr. *N. natrix*, all of them hygrophilous and/or generalist taxa, tolerant to wet Mediterranean conditions. A third group comprised *P. syriacus*, *Bu. viridis* gr., *Mauremys* sp., *Blanus* sp. and *Coronella* cf. *C. austriaca*, which showed a low similarity ratio. This group combined species of native European species tolerant to Eurosiberian conditions with other taxa from eastern origins. Finally, *Hyla* gr. *H. arborea* appeared in a marginal position outside the rest of the cluster.

In the case of the assemblages (Fig. S1B), the hierarchical cluster (*cophen. corr.* = 0.8376) showed two major clades, in turn divided into subclades. The first major clade was dominated by the taxa *Lacerta* s.l. and cf. *Podarcis* sp., and was formed by PN6, PN15, PN18, PN22 in posto, PN34 err, PN34c, and PN34d; the second major clade was dominated by associations with a greater number of taxa in concurrence, particularly the first subclade was formed by PN1, PN5, PN9, PN11, PN13, PN16 and PN17, in which most of the hygrophilous taxa (mainly *Bufo* gr. *B. bufo*, *Hyla* gr. *H. arborea*, *Natrix* gr. *N. natrix*, *Coronella* cf. *C. austriaca*, *H. viridiflavus*, and *Zamenis* gr. *Z. longissimus*) were recorded in concurrence with the rest of the dominant taxa of Pirro Nord (*Pelophylax* sp., *E. orbicularis*, *T. hermanni*, cf. *Podarcis* sp. and *Lacerta* s.l.), which in turn formed almost exclusively the second subclade constituted by PN2, PN5b, PN12, PN25, PN26 and PN34a.

The correspondence analysis also presented a triple grouping (Fig. 8), but differed in the organization of the taxa. In its graphical representation, the terrestrial taxa appeared in the upper half while the main aquatic taxa (*Pelophylax* sp. and *E. orbicularis*) were in the lower positions. Likewise, among the terrestrial taxa there was a clear differentiation between the more heliophiles and those that prefer open habitats (cf. *Podarcis* sp. and *Lacerta* s.l.), located in the left section of the graph, in front of the more typical of wetter habitats and/or with a greater vegetal coverage (*Bufo* gr. *B. bufo*, *Hyla* gr. *H. arborea*, *Mauremys* sp., *Natrix* gr. *N. natrix*, *Coronella* cf. *C. austriaca*, *Zamenis* gr. *Z. longissimus* and *H. viridiflavus*), which appeared in the upper right side. In contrast, *T. hermanni* was in an eccentric position, within the group of dominant aquatic taxa. In the analysed sites of Pirro Nord, the two freshwater terrapin taxa (*E. orbicularis* and *Mauremys* sp.), when both appeared in the data matrix, always co-occurred with *T. hermanni*. This was the case with *E. orbicularis* from PN1, PN2, PN5, PN13, PN16, PN22err, PN26 and PN32; and with *Mauremys* sp. from PN2, PN11 and PN13. The same is true for the frog *Pelophylax* sp. from Pirro Nord, whose remains have also been recorded in concurrence with *T. hermanni* in PN1, PN2, PN5b, PN9, PN13, PN16, PN17, PN22err, PN25 and PN34a. *P. syriacus* and *Blanus* sp. exhibited extreme positions, close to hygrophilous taxa, due to their environmental preferences for dry habitats with loose substrates. A palaeoecological characterisation for the herpetological concurrences of the Pirro Nord sites can be observed in the axes of the correspondence analysis graph, where the horizontal axis corresponds to a gradient from heliophilia to hygrophilia, while the horizontal axis from terrestrial to aquatic trends.

3.5. Statistical analyses

Statistical analyses following the rarefaction and extrapolation with

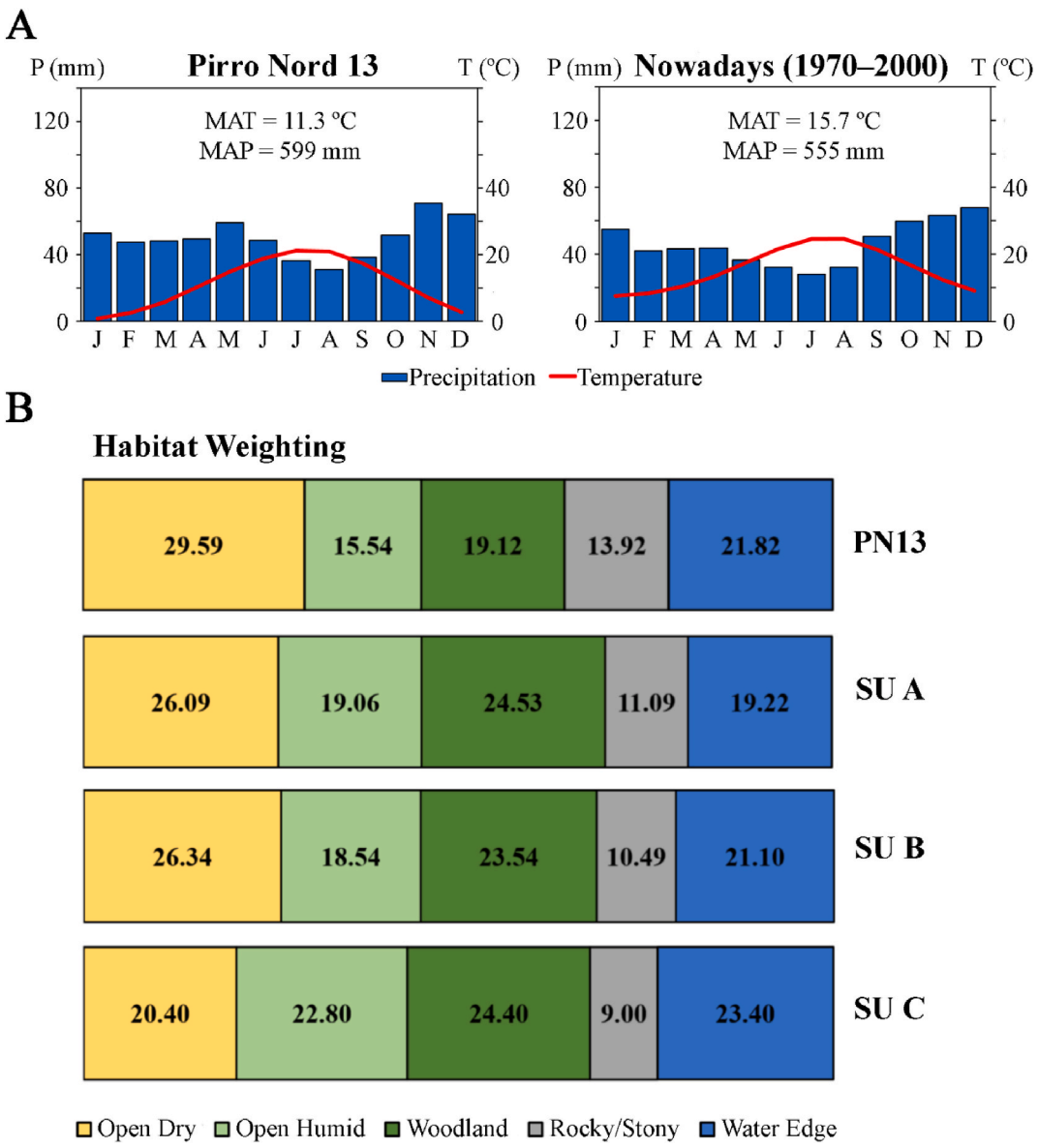

Fig. 7. Quantitative palaeoecological reconstructions of the Early Pleistocene site of Pirro Nord 13 (PN13; Apricena, southern Italy). **A**, Climatograms corresponding to the quantitative climate reconstruction of PN13, resulting from the MER (Mutual Ecogeographic Range) method and the UDA-ODA (Uncertain Distribution Area-Occupied Distribution Area) discrimination technique; plus the modern climate values of the PN13 site location nowadays (1970–2000; data from WorldClim 2.1, Fick and Hijmans, 2017). In both cases the scale P = 2 x T was applied. **B**, Palaeoenvironmental reconstructions resulting from the Habitat Weighting method, applied considering PN13 as a whole, and separately to the different Stratigraphic Units with a sufficient number of remains (SU A, SU B, and SU C). Values for habitat weightings are in percentages (%). Abbreviations: P = precipitation, T = temperature, MAT = mean annual temperature, MAP = mean annual precipitation, SU = Stratigraphic Unit.

Hill numbers method allowed testing sample completeness and comparing biodiversity between assemblages. The selected base sample size (*m*) is 103, being the maximum reference sample size of the analysed assemblages (PN13).

Comparing diversity among sites based on sample-size (Fig. S2A; Table S5), in terms of species richness (q = 0), the PN9 and PN16 sites were distinguishable from the others, exhibiting the highest values (24.84 and 24.41, respectively). The other sites appeared closer to each other, forming three groups. The first one comprises PN1, PN13 and PN17 sites, which had richness values of 19.92, 13.00, and 12.37, respectively. The second group, occupying an intermediate position, was composed of PN5 and PN11 sites, which had richness values of 9.64 and 9.13, respectively. The third group corresponds corresponded to the less rich assemblages, and was composed by PN2, PN5B and PN12 sites, which had richness values of 6.48, 5.48, and 5.87, respectively. However, despite the observed differences in species richness between the analysed sites, these differences were not statistically significant (95 % confidence intervals overlapped).

According to Shannon and Simpson indices (q = 1 and q = 2, respectively; Fig. S2A; Table S5), PN5, PN5B and PN12 sites were less diverse in terms of evenness than the other ones (evenness values of 3.48, 3.76, and 2.26, respectively). This fact was because PN5 and PN12 assemblages were dominated by cf. *Podarcis* sp., and PN5B by *Lacerta* s.l. In the other assemblages, the species were more equally distributed. The PN16 site exhibited the highest value of evenness (25.88).

The results obtained were then compared with coverage-based rarefaction and extrapolation curves (Fig. S2B; Table S6), which confirmed the order and significance of the biodiversity indices between the analysed assemblages detected in the sample-size based curves (Fig. S2A). Both type of curves were linked with the construction of a

Table 4
Climatic interpretation for the Early Pleistocene site of Pirro Nord 13 (Apricena, southern Italy) and modern climate (1970–2000). Abbreviation: MTC = mean temperature of the coldest month.

	Pirro Nord 13		Nowadays (1970–2000)	
Mean annual temperature	11.3 °C	cold	15.7 °C	warm
Atmospheric temperature range	20.5 °C	very high	17.1 °C	high
Summer temperature	0 months > 22 °C	warm-temperate	2 months > 22 °C	warm
Winter temperature	MTC = 0.8 °C	cold	MTC = 7.6 °C	temperate
Mean annual precipitation	599.4 mm	low	554.8 mm	low
Distribution of rainfall	regular		fairly regular	winter
Type of precipitation	rain		rain	
Gaussen Index	2	Continental	3	Mediterranean
Lautensach-Mayer Index	2	semi-humid	3	semi-humid
Dantin-Revenga Index	1.8	humid	2.8	semi-arid
De Martonne Index	28.2	semi-humid	21.6	semi-humid

sample completeness curve (Fig. S2C), which allowed us to examine how the sample completeness varied with the sample size. When the sample size was standardised, there were no differences in terms of sample coverage. All the analysed sites exhibited high values, comprised between 0.9 and 1 (Tables S5 and S6), with not statistically significant differences between them (95 % confidence interval fully overlaped). These results provided a statistical validation about the consistency of both curve types (i.e., sample-size and sample-coverage based curves).

4. Discussion

The evolution and dispersal of early hominins over the last 2 Ma have been said to be specially influenced by climatic and environmental changes (e.g., Agustí et al., 2009; deMenocal, 2011; Timmermann et al., 2022, 2024), which affected resource availability and the distribution, size, and connectivity of habitable areas (Mondanaro et al., 2020; Potts, 1998; Potts et al., 2020; Timmermann et al., 2024). Understanding the ecological circumstances under which the first human dispersals into the Eurasian continent occurred can, thus, shed light on early hominin capacities and behaviours.

It now seems well established that the first known dispersal of early hominins inside Eurasia was accompanied by niche expansion (see Blain et al., 2021; Foister et al., 2023, 2024; Potts, 2002; Timmermann et al., 2022, 2024). As early hominins dispersed into the Eurasian continent, they encountered and successfully adapted to environments that differed from those they had left behind in Africa (Agustí and Lordkipanidze, 2019; Foister et al., 2023, 2024; Saarinen et al., 2021; Zeller et al., 2023). However, the understanding of this climate forcing on early hominins has been hindered by the limited spatial resolution and temporal continuity of the archaeological record, as well as by the scarcity of information on past vegetation and ecosystem changes near archaeological sites (see Zeller et al., 2023). In this regard, regional-scale studies based on different palaeoecological proxies (e.g., pollen, large herbivores, small vertebrates), provide a complementary perspective to global-scale studies and highlight the importance of considering the diversity of microhabitats within a given region when studying species dispersal dynamics (e.g., Blain et al., 2019; Domínguez-García et al., 2024; Ochando et al., 2022; Ramírez-Pedraza et al., 2024; Saarinen et al., 2021; Sánchez-Bandera et al., 2020, 2023). These methodological approaches facilitate the analysis of the diverse habitats and climates that early hominins encountered during their dispersals across Eurasia. Moreover, they enable the characterisation of those ecological moments within the Early Pleistocene climate variability. This, in turn, facilitates a better understanding of the processes involved in adaptation and the relative suitability of those ecological scenarios.

Our study presents a quantitative palaeoecological analysis of the Early Pleistocene site of Pirro Nord 13, based on its herpetofaunal assemblage. Owing to their strong dependence on climatic and environmental conditions, amphibians and reptiles serve as reliable ecological indicators. Furthermore, their spatial association with human evidence at the site enables a direct link between reconstructed ecological conditions and early hominin activities. The methodological approach employed allows for the generation of robust, quantitative palaeoecological reconstructions, thereby minimising interpretative biases typically associated with qualitative analyses (see Foister et al., 2023). This framework enhances the comparability of our results with other palaeoecological datasets and contributes to a more refined understanding of the climatic and environmental context of early hominins.

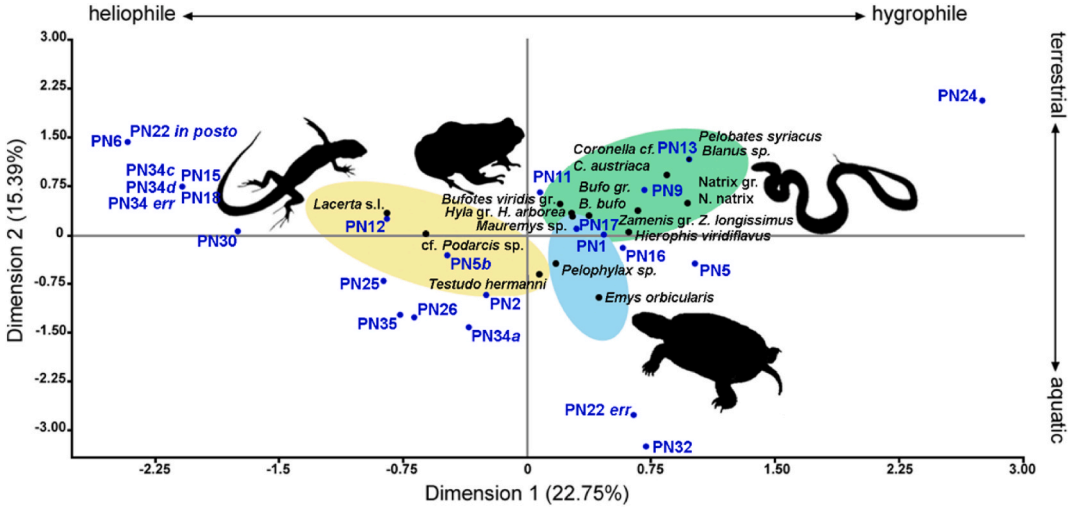

Fig. 8. Graphic representation of the correspondence analysis (CA) of fossil herpetological assemblages from the Pirro Nord sites of PN1, PN2, PN5, PN5b, PN6, PN9, PN11, PN12, PN13, PN15, PN16, PN17, PN18, PN22err, PN22 in posto, PN22bis, PN24, PN24b, PN25, PN26, PN30, PN32, PN34err, PN34a, PN34c, PN34d and PN35. The yellow ellipse corresponds to the heliophilic species association; the blue ellipse the aquatic species association; and the green ellipse the hygrophilic species association.

4.1. Amphibian and reptile assemblage of PN13

The herpetofaunal assemblage of PN13 was clearly dominated by reptiles, both in terms of the numbers of remains (MNE) and the number of individuals identified (MNI). Among the reptile taxa, the colubrid *Zamenis* gr. *Z. longissimus* stood out in terms of number of remains, and cf. *Podarcis* sp. in terms of the number of individuals identified (Table 1). The high number of chelonian elements identified (especially in the case of *Testudo hermanni*) in relation to the other taxa may be due to a taphonomic bias, i.e. as could be the greater probability of preservation of chelonian remains in the fossil record compared to other species of herpetofauna, due to the greater robustness of their skeletal elements. Amphibians were only represented by anurans, consisting of three species of toads (*Pelobates syriacus*, *Bufotes viridis* gr., and *Bufo* gr. *B. bufo*), and one frog (*Pelophylax* cf. *esculentus/ridibundus*). Among them, *Bu. viridis* gr. is clearly dominant, being the most represented taxon of the assemblage both in terms of MNE and MNI (Table 1). The other three anurans were equally represented.

At the biogeographical level, all the taxa documented in the fossil record of PN13 are currently present in southern Italy (see Sindaco et al., 2009), with the exception of *P. syriacus*, *Mauremys* sp. and *Blanus* sp. (Table S1).

In the Italian Peninsula the genus *Pelobates* is currently only represented by *Pelobates fuscus*, found in the northern area on the Po Plain (Lanza et al., 2007; Sindaco et al., 2009). The taxon *P. syriacus* is currently living in the southeastern Balkan Peninsula, Caucasus and the Middle East. Its documentation in PN13 corresponds to the only record of this species in the Apennine Peninsula (Blain et al., 2016b).

Mauremys is a genus of freshwater terrapin that is currently locally extinct in the Apennine Peninsula (see Chesi et al., 2007) but represented elsewhere in Southern Europe by two species: in the Iberian Peninsula by *Mauremys leprosa*, an Iberian-Maghrebian species, whereas *Mauremys rivulata* is distributed in the south of the Balkan Peninsula and western Anatolia (Fritz et al., 2008).

The worm-lizards of the genus *Blanus* are also absent from the Apennine Peninsula (see Delfino, 1997). The distribution of this genus is currently disjunctive, showing a widely fragmented range: the *Blanus cinereus* complex is present in the western Mediterranean regions (including the Iberian species *Bl. cinereus* and *Blanus oxyurus*, and the Maghrebian species *Blanus metteali* and *Blanus tingitanus*; Albert et al., 2007; Sánchez-Vialas et al., 2024), while the *Blanus strauchi* complex (including *Bl. s. strauchi*, *Blanus s. bedriagae*, *Blanus aporus*, and *Blanus alexandri*) is present in the eastern Mediterranean area, being currently distributed in southern Anatolia, on islands in the southern Aegean Sea, in Iraq, Syria, Lebanon, and northern Israel (Sindaco et al., 2014).

The climatic changes along the Quaternary and the consequent changes in the distribution of the species could explain the arrival of eastern herpetofauna to the southern regions of the Apennine Peninsula, especially of *Ma. rivulata* from the Balkan Peninsula. The successive decreases in sea level during the Quaternary glacial periods diminished the distance between the emerged continental masses from the Apennine Peninsula and the western Balkans, until being separated only by a small marine basin, the "Mid Adriatic Pit" or "Meso Adriatic Depression" (Correggiari et al., 1996), which may have favoured an expansive distribution of *Ma. rivulata* and other eastern species towards the west in a similar way to the colonization through the Strait of Gibraltar by *Ma. leprosa*, from north-western Maghreb to the Iberian Peninsula (Velo-Antón and Pinya, 2015).

4.2. Comparison with other proxies at PN13

The Pirro Nord sites have been analysed palaeoecologically based on the large mammal, bird, and herpetofaunal assemblages (Pavia et al., 2012; Blain et al., 2019). In general, all these studies indicate open and dry environments, with colder climatic conditions than those observed today in the area. Nevertheless, the palaeoecological conditions of the PN13 site remained to be fully explored. To date, only Berto et al. (2024) proposed quantitative palaeoenvironmental and palaeoclimatic reconstructions for PN13 (SU D) based on the small mammal assemblage. Environment was reconstructed as mainly open, with a patch of mixed forest cover, while the rocky and aquatic components are almost absent. The climatic conditions were reconstructed as mildly colder and more humid than present day ones, and with similarities to the modern Mediterranean climate.

The palaeoenvironmental data obtained with the herpetofaunal assemblage aligned with this landscape reconstruction, except for the aquatic component that is well represented in our reconstruction, as evidenced by the occurrence of the Testudines taxa *Emys orbicularis* and *Mauremys* sp., and the green frog *Pelophylax* cf. *esculentus/ridibundus* In the case of the small mammals, the only identified taxon strictly related with aquatic habitats is *Asoriculus* sp. Our results also agreed with Berto et al. (2024) who obtained 25.8 % of representation for woodland habitats around PN13. This presence of woodland areas can be put in relation to the closest pollen core reported in the Early Pleistocene site of Petrafitta (Umbria, central Italy), with a synchronous age (dated to ca. 1.6–1.4 Ma), which indicate the presence of 'scattered' forested zones (Lona and Bertoldi, 1973; Leroy et al., 2011). However, it is to stress that no taxa strictly related to woodland (e.g. suids, glirids, forest birds, or brown frogs) have ever been recorded in the Pirro Nord complex.

Moreover, our data indicate colder and more continental conditions than those suggested by Berto et al. (2024). The inferred MAT based on small mammals is reconstructed to be 3.7 °C warmer, and MAP 355 mm higher in relation to our results based on herpetofauna. However, when considering the standard deviation, it is considerably wide for the small mammal reconstruction, and encompasses our results for both variables (Fig. S3). The observed discrepancies between the two climatic data sets may be attributable to the divergent methodologies employed, in addition to the inherent characteristics of the proxy in question (herpetofauna and small mammals). The Bioclimatic Model method employed by Berto et al. (2024) has been demonstrated to be less precise than the MER/ODA methodology, due to differences in the nature of the data (see Fagoaga et al., 2023 for further explanation). Despite these methodological differences between the two palaeoclimatic reconstructions, a concordant tendency is nevertheless observed, thereby demonstrating some agreement between them.

4.3. Comparison between PN13 and other deposits from Pirro Nord

Palaeoecological reconstructions of some of the other fissures of the Pirro Nord complex (Blain et al., 2019) have led to the differentiation between sites exhibiting temperatures lower than present and displaying heliophilic taxa associations more characteristic of open environments (sites PN2, PN5b, PN11, PN12), and sites with temperatures more similar to present ones, exhibiting hygrophilic associations more characteristic of forested or humid environments (sites PN1, PN5, PN9, PN16, PN17). The PN13 site is located between both groups, as demonstrated also by the species diversity analysis (Fig. S2). The reconstructed temperatures at the PN13 site are colder than present day, similar to the first group values. However, the species assemblage is more diverse and includes a greater number of hygrophilic species. This observation is further corroborated by the Habitat Weighting results, which show a potentially good representation of the woodland habitat component.

The differences between the identified herpetofaunal fossil assemblages and species interrelationship analyses help to better understand the diverse environmental conditions detected (Fig. 8 and S1). The dominance in the fossil record of the thermophilic and/or heliophilic taxa *T. hermanni*, cf. *Podarcis* sp., *Lacerta* s.l., and in minor representation by *Blanus* sp., points to the existence of large open spaces, with low vegetation and or stony, with a high level of insolation. The presence of freshwater points is indicated by the record of the aquatic taxa *Pelophylax* sp., *Mauremys* sp. and *E. orbicularis*, as well as temporary water

points by *Bu. viridis* gr. and *P. syriacus*. To a lesser extent, there would be environments with a greater vegetation coverage and higher environmental humidity, such as riverside forests or humid meadows, where taxa of comparatively more hygrophilic preferences would appear, such as *Hyla* gr. *H. arborea*, *Bufo* gr. *B. bufo*, *Natrix* gr. *N. natrix*, *Hierophis viridiflavus*, and *Zamenis* gr. *Z. longissimus*.

The statistical results obtained by the rarefaction and extrapolation with Hill numbers method (see Fig. S2; Tables S5 and S6), guarantee that the observed palaeoclimatic and palaeoenvironmental differences between the compared sites (i.e., PN1, PN2, PN5, PN5B, PN9, PN11, PN12, PN13, PN16, and PN17) are not caused by differences in the size or coverage of the respective fossil assemblages.

4.4. PN13 inside the early Pleistocene climate variability

The climate during the Early Pleistocene was driven by astronomical-obliquity-dominated 'glacial'-'interglacial' cycles lasting 41 ka (Lisiecki and Raymo, 2005), which resulted in 42 successive cycles of corresponding vegetation, ranging from open landscapes (during 'glacial' periods) to dense forest landscapes (during 'interglacial' periods) (Leroy et al., 2011). The 'interglacial' periods were characterised by higher temperatures and precipitation compared to the present-day conditions, whereas the 'glacial' periods were marked by shorter durations and non-extreme conditions, with temperatures and precipitation values similar to modern ones. These 'glacial' periods during the Early Pleistocene were also characterised by the presence of open landscapes and open forest, rather than steppe-like landscapes (Altolaguirre et al., 2019).

The reconstructed cold and dry conditions for PN13 can be attributed to an Early Pleistocene 'glacial' period. This attribution is further substantiated by the palaeoenvironmental reconstructions, which indicate a predominance of open and dry landscapes.

To better understand the contextualization of the palaeoecological conditions of PN13 inside the Early Pleistocene climate variability, we integrated our obtained data with the adapted Early Pleistocene 'glacial-interglacial vegetation cycle' model developed by Sánchez-Bandera et al. (2023). This cyclic model shows: 1) a pre-temperate cool and dry phase of open woodland, 2) a temperate phase characterised by an early expansion of deciduous forests, 3) a post-temperate cool and drier phase of open woodland, and 4) the installation of a cold and dry 'glacial'--steppe phase.

When considering this model, PN13 can be situated within a cool and humid phase, in the transition from a warm and humid temperate phase toward a cool and humid post-temperate phase. During this transition from an 'interglacial' to a 'glacial' climatic period, the landscape was more forested than during the transition from a 'glacial' to an 'interglacial' period (Leroy and Ravazzi, 1997; Leroy et al., 2011).

In our reconstructed environment for PN13, the forest component is relatively well represented (19.12 % of the landscape; Fig. 7B; Table 3), indicated also by the presence of species with hygrophilic preferences in the assemblage (Fig. 8). This forest component representation is higher than that expected for a drier and more open landscape, which would occur during the transition from 'glacial' to 'interglacial' periods.

4.5. Implications for the early hominin ecological niche

The range of climatic and environmental values for the occurrence of early hominins in western Eurasia has recently been estimated by Blain et al. (2021), who proposed an ecological model based on a database developed for 23 Early and Middle Pleistocene sites in Spain. This model is referred to as the 'Iberian' ecological model. These authors proposed that a climatic constraint affected human settlement expansion beyond the African continent and is related to rainfall and environmental humidity (expressed as forest cover), more than other factors such as temperature. An analysis of major Spanish palaeoanthropological sites exhibited MAT that does not fall below 8.4 °C, mean temperature of the warmest month (MTWM) ranging from 16.4 to 27.5 °C, and a mean temperature of the coldest month (MTCM) ranging from 0.5 to 12.0 °C. These sites also exhibit a MAP that exceeds 732 mm, along with a forest cover (% wood) ranging from 26.0 to 41.5 % of the total landscape.

Our climate and environmental estimates for PN13 are consistent with the proposed model in terms of temperature, which falls within the specified range. However, the values for MAP and % wood are lower than those suggested by the model (Table 5). This discrepancy could indicate that the palaeoclimatic and palaeoenvironmental conditions at PN13, although still favourable for hominin presence, were globally challenging for these early hominins, even if the scarcity of rainfall during most of the year would have been locally compensated by the presence of freshwater environments (rivers or lakes), as evidenced by the presence of aquatic the taxa such as *Emys orbicularis*, *Mauremys* sp. and *Pelophylax* cf. *esculentus/ridibundus*.

The comparison of the palaeoecological data estimated for PN13 with the warm, humid and more forested reconstructions for the older early hominin site of Dmanisi (ca. 1.8 Ma, Georgia, Lesser Caucasus; Blain et al., 2022) and the younger one of Barranco León (ca. 1.4 Ma, Guadix-Baza Basin, southeastern Spain; Sánchez-Bandera et al., 2020, 2023) suggests the presence of a globally colder and drier period in between (attributable to the 'phase 2' described by Agustí et al., 2009). Such a period may have delayed the hominin dispersal into Europe.

These cold and drier conditions, which could have been challenging for early hominins, have also been documented in the level 5 of the younger site of Fuente Nueva 3 (ca. 1.2 Ma, Guadix-Baza Basin, southeastern Spain; Sánchez-Bandera et al., 2020, 2023). This Iberian locality, however, exhibits warmer temperatures (+3.4 °C), similar precipitation values (+19 mm), and almost no forest coverage, which is consistent with the major role of the precipitation and the environmental humidity during the early hominin dispersals, as suggested by the 'Iberian' ecological model (Blain et al., 2021).

The new palaeoecological reconstructions for PN13 provide substantial information regarding the ecological tolerances of the early hominins, suggesting that they were capable of coping with challenging climatic and environmental conditions. It is noteworthy that in both cases (Fuente Nueva 3 and PN13), these hominin sites are located in the southern regions of Mediterranean peninsulas (specifically, the Iberian and Italian peninsulas). This may be due to the difficulties of reaching northern areas and moving across the European continent during these colder and drier ('glacial'-like) phases.

Furthermore, within the context of human dispersals across the European continent, our data contribute to the current knowledge gap between eastern European early hominin sites (e.g. Grăunceanu, Dmanisi, and Korolevo) and western sites (e.g. Barranco León, Fuente Nueva 3, and Sima del Elefante TE7).

5. Conclusions

In this study, we described for the first time the fossil amphibians and reptiles from the Early Pleistocene site of PN13, hosted at the Museo di Geologia e Paleontologia collections (MGPT-PU) of the Torino University (Turin, Italy), and used them to perform new quantitative palaeoecological reconstructions. The results provide valuable insights into the ecological tolerance of early hominins, improving our understanding of their distribution and the delays observed in their dispersal across the European continent. The conclusions are as follow.

1. The PN13 climate is reconstructed as cold and humid/semi-humid, similar to the present-day continental Mediterranean climate. The surrounding landscape was dominated by open environments, primarily composed of open-dry habitats, with the presence of woodland areas along water bodies or temporary swamps.
2. These climatic and environmental conditions can be related with a cold and dry period ('glacial'), which would have occurred during a post-temperate phase ('interglacial' to 'glacial' transition) within the

Table 5
Comparison between the palaeoecological parameters reconstructed for the Early Pleistocene site of Pirro Nord 13 (Apricena, southern Italy) and the 'Iberian' ecological model (Blain et al., 2021). In both cases Min and Max values correspond to the mean ± standard deviation. Abbreviations: MAT = mean annual temperature, MTCM = mean temperature of coldest month, MTWM = mean temperature of warmest month, MAP = mean annual precipitation, Min = minimum, Max = maximum.

	MAT (°C)		MTCM (°C)		MTWM (°C)		MAP (mm)		% wood	
	Min	Max	Min	Max	Min	Max	Min	Max	Min	Max
'Iberian' ecological model	8.4	18.5	0.5	12.0	16.4	27.5	732	1242	26.0	41.5
Pirro Nord 13	9.6	13	−0.7	2.3	19.3	23.1	533	665	19.12	

variability of the Early Pleistocene climate, when the forested landscapes still persisted.
3. These new estimates are consistent with previous reconstructions based on small-mammals, which suggested mildly colder and more humid climatic conditions than that of present-day, and corroborated the presence of open environments with a patch of mixed forest cover.
4. In comparison to other sites of the Pirro Nord locality, PN13 occupies an intermediate position in terms of both climate and environmental conditions. PN13 is positioned between the more forested and humid sites, which exhibit temperatures similar to present-day, and those with drier environments and colder than present temperatures.
5. The cold and dry climatic scenario inferred at PN13 differs to the proposed favourable ecological conditions for early hominins, suggesting that they were capable of coping with challenging climatic and environmental conditions. This discrepancy could explain the delays observed in the hominin dispersal into the European continent, as in the case evidenced between ca. 1.8 and 1.4 Ma.

Author statement

Christian Sánchez-Bandera: Data curation; Formal analysis; Investigation; Methodology; Visualization; Writing – original draft. **Hugues-Alexandre Blain:** Conceptualization; Funding acquisition; Investigation; Project administration; Supervision; Writing – original draft. **Josep Francesc Bisbal-Chinesta:** Formal analysis; Writing – original draft. **Ana Fagoaga:** Methodology; Supervision; Validation; Writing-Review and Editing. **Marco Pavia:** Resources; Writing-Review and Editing. **Massimo Delfino:** Writing-Review and Editing.

Declaration of competing interest

The authors declare that they have no known competing financial interests or personal relationships that could have appeared to influence the work reported in this paper.

Acknowledgements

This publication is part of the R&D&I project PID2021-122533NB-I00 "Using climate envelope models to predict spatial and temporal distribution patterns of climate-related Quaternary extinctions", funded by MCIN/AEI/10.13039/501100011033/and by ERDF, EU, and the Leakey Fundation Project "Early hominin climate envelope: The lower vertebrate perspective". C.S.-B is supported by a FPI Predoctoral Scholarship (PRE2020-094482) associated with project CEX2019-000945-M-20-1 with the financial sponsorship of the Spanish Ministry of Science and Innovation and co-financed by the European Social Fund. A.F. is supported by a Margarita Salas contract (MS21-048) from the 'Ayudas para la recualificación del sistema universitario español', Spanish Ministerio de Universidades, financed by the European Union, NextGenerationEU. C.S.-B. and H.-A.B. belongs to the Consolidated Research Group "Paleoecology of Pliocene and Pleistocene and Human Dispersals (PalHum)", funded by AGAUR-Generalitat de Catalunya, 2021SGR-1238 and URV 2023PFR-URV-01238. The Institut Català de Paleoecologia Humana i Evolució Social (IPHES-CERCA) received financial support from the Spanish Ministry of Science and Innovation through the "María de Maeztu" program for Units of Excellence (CEX2019-000945-M). We are grateful to Dr. Rebecca Biton for providing us with her research data on the Testudines of PN13. C.S.-B. would like to express his gratitude to Dr. Alexia Serrano-Ramos (Universidad de Granada, Spain) for her valuable assistance with the database management. We are also grateful to the editor Prof. Rivka Rabinovich and two anonymous for valuable comments and suggestions on our manuscript. This is the publication number 380 of the Museo di Geologia e Paleontologia collections at the Universita degli Studi di Torino.

Appendix A. Supplementary data

Supplementary data to this article can be found online at https://doi.org/10.1016/j.quascirev.2025.109555.

Data availability

Data are available at the following link: https://doi.org/10.34810/data2091 (Sánchez-Bandera et al., 2025).

References

Abbazzi, L., Benvenuti, M., Boschian, G., Dominaci, S., Masini, F., Mezzabotta, C., Rook, L., Valleri, G., Torre, D., 1996. The Neogene and Pleistocene succession and the mammal faunal assemblages of an area between Apricena and Poggio Imperiale (Foggia). Mem. Soc. Geol. Ital. 51, 383–402.

Agustí, J., Lordkipanidze, D., 2019. An alternative scenario for the first human dispersal out of Africa. L'Anthropologie 123 (4–5), 682–687. https://doi.org/10.1016/j.anthro.2019.102727.

Agustí, J., Blain, H.-A., Cuenca, G., Bailon, S., 2009. Climate forcing of first hominid dispersal in Western Europe. J. Hum. Evol. 57, 815–821. https://doi.org/10.1016/j.jhevol.2009.06.005.

Agustí, J., Blain, H.-A., Furió, M., De Marfà, R., Santos-Cubedo, A., 2010. The early Pleistocene small vertebrate succession from the Orce region (Guadix-Baza Basin, SE Spain) and its bearing on the first human occupation of Europe. Quat. Int. 223–224, 162–169. https://doi.org/10.1016/j.quaint.2009.12.011.

Agustí, J., Leroy, S.A.G., Lozano-Fernández, I., Ramón, J., 2018. Joint vegetation and mammalian records at the early Pleistocene sequence of Bòvila Ordis (Banyoles-Besalú Basin, NE Spain) and their bearing on early hominin occupation in Europe. Palaeobiodivers. Palaeoenviron. 98, 653–662. https://doi.org/10.1007/s12549-018-0324-5.

Albert, E.M., Zardoya, R., García-París, M., 2007. Phylogeographical and speciation patterns in subterranean worm lizards of the genus *Blanus* (Amphisbaenia: blanidae). Mol. Ecol. 16 (7), 1519–1531. https://doi.org/10.1111/j.1365-294X.2007.03248.x.

Altolaguirre, Y., Postigo-Mijarra, J.M., Barrón, E., Carrión, J.S., Leroy, S.A.G., Bruch, A. A., 2019. An environmental scenario for the earliest hominins in the Iberian Peninsula: early Pleistocene palaeovegetation and palaeoclimate. Rev. Palaeobot. Palynol. 260, 51–64. https://doi.org/10.1016/j.revpalbo.2018.10.008.

Arnold, E.N., Burton, J.A., 1978. Guía De Campo De Los Reptiles Y Anfibios De España Y De Europa. Editorial Omega, Barcelona.

Arntzen, J.W., Recuero, E., Canestrelli, D., Martínez-Solano, I., 2013. How complex is the *Bufo bufo* species group? Mol. Phylogenet. Evol. 69, 1203–1208. https://doi.org/10.1016/j.ympev.2013.07.012.

Arzarello, M., Marcolini, F., Pavia, G., Pavia, M., Petronio, C., Petruci, M., Rook, L., Sardella, R., 2007. Evidence of earliest human occurrence in Europe: the site of Pirro Nord (Southern Italy). Naturwissenschaften 94, 107–112. https://doi.org/10.1007/s00114-006-0173-3.

Arzarello, M., Marcolini, F., Pavia, G., Pavia, M., Petronio, C., Petrucci, M., Rook, L., Sardella, R., 2009. L'industrie lithique du site Pléistocène inférieur de Pirro Nord (Apricena, Italie du sud) : une occupation humaine entre 1,3 et 1,7 Ma. L'Anthropologie 113 (1), 47–58. https://doi.org/10.1016/j.anthro.2009.01.004.

Arzarello, M., Pavia, G., Peretto, C., Petronio, C., Sardella, R., 2012. Evidence of an early Pleistocene hominin presence at Pirro Nord (Apricena, Foggia, southern Italy): P13 site. Quat. Int. 267, 56–61. https://doi.org/10.1016/j.quaint.2011.01.042.

Arzarello, M., Peretto, C., Moncel, M.-H., 2015. The Pirro Nord site (Apricena, Fg, Southern Italy) in the context of the first European peopling: convergences and divergences. Quat. Int. 389, 255–263. https://doi.org/10.1016/j.quaint.2014.08.051.

Bailon, S., 1991. Amphibiens Et Reptiles Du Pliocène Et Du Quaternaire De France Et D'Espagne: Mise En Place Et Évolution Des Faunes. Unpublished PhD thesis, Université de Paris VII, Paris.

Bailon, S., 1999. Différenciation ostéologique des anoures (Amphibia, Anura) de France. In: Desse, J., Desse-Berset, N. (Eds.), Fiches D'Ostéologie Animale Pour L'Archéologie, Série C Varia. Valbonne: Centre de Recherches Archéologiques-CNRS, p. 38.

Bagnus, C., 2011. Analisi Tafonomica Delle Associazioni a Vertebrati Del Pleistocene Inferiore Di Pirro Nord. Turin.

Barahona Quintana, F.F., 1996. Osteología craneal de Lacértidos de la Península Ibérica e Islas Canarias: análisis sistemático filogenético. Ph.D Dissertation, Universidad Autónoma de Madrid.

Barahona, F., Barbadillo, L.J., 1997. Identification of some Iberian lacertids using skull characters. Rev. Espanola Herpetol. 11, 47–62.

Barsky, D., Titton, S., Sala-Ramos, R., Bargalló, A., Grégoire, S., Saos, T., Serrano-Ramos, A., Oms, O., Solano García, J.-A., Toro-Moyano, I., Jiménez-Arenas, J.M., 2022. The significance of subtlety: contrasting lithic raw materials procurement and use patterns at the Oldowan sites of Barranco León and fuente Nueva 3 (Orce, Andalusia, Spain). Front. Earth Sci. 10. https://doi.org/10.3389/feart.2022.893776.

Bisbal-Chinesta, J.F., Blain, H.-A., 2018. Long-term changes in composition and distribution patterns in the Iberian herpetofaunal communities since the latest Pleistocene. Quat. Sci. Rev. 184, 143–166. https://doi.org/10.1016/j.quascirev.2017.06.010.

Berruti, G.L.F., 2017. Use-wear analysis of discoid-conception lithic industries. Universidade de Trás-os-Montes e Alto Douro, Vila Real.

Berruti, G.L.F., Arzarello, M., 2020. Talking stones: taphonomy of the lithic assemblage of Pirro Nord 13 (Apricena, FG, Italy). A new approach to the study of the post depositional alterations on lithic tools. J. Archaeol. Sci. Rep 31, 102282. https://doi.org/10.1016/j.jasrep.2020.102282.

Berto, C., Arnaud, J., López-García, J.M., Luzi, E., Arzarello, M., 2024. Analysis of the Early Pleistocene small mammals from Pirro Nord 13 (Apricena, southern Italy) and their implications for reconstructing the palaeoenvironment of the early human occupation in Europe. Palaeogeogr. Palaeoclimatol. Palaeoecol. 647, 112251. https://doi.org/10.1016/j.palaeo.2024.112251.

Blain, H.-A., Bailon, S., Agustí, J., 2007. Anurans and squamate reptiles from the final Early Pleistocene of Almenara-Casablanca-3 (Castellón, East of Spain). Systematic, climatic and environmental considerations. Geodiversitas 29, 269–295.

Blain, H.-A., Bailon, S., Cuenca-Bescós, G., 2008. The early–middle Pleistocene palaeoenvironmental change based on the squamate reptile and amphibian proxy at the Gran Dolina site, Atapuerca, Spain. Palaeogeogr. Palaeoclimatol. Palaeoecol. 261, 177–192. https://doi.org/10.1016/j.palaeo.2008.01.015.

Blain, H.-A., Lozano-Fernández, I., Böhme, G., 2015. Variation in the ilium of central European water frogs *Pelophylax* (Amphibia, Ranidae) and its implications for species-level identification of fragmentary anuran fossils. Zool. Stud. 54 (1), 5. https://doi.org/10.1186/s40555-014-0094-3.

Blain, H.-A., Lozano-Fernández, I., Agustí, J., Bailon, S., Menéndez Granda, L., Espígares Ortiz, M.P., Ros-Montoya, S., Jiménez Arenas, J.M., Toro-Moyano, I., Martínez-Navarro, B., Sala, R., 2016a. Redefining upon the climatic background of the early Pleistocene hominid settlement in western Europe: Barranco León and Fuente Nueva-3 (Guadix-Baza Basin, SE Spain). Quat. Sci. Rev. 144, 132–144. https://doi.org/10.1016/j.quascirev.2016.05.020.

Blain, H.-A., Delfino, M., Berto, C., Arzarello, M., 2016b. First record of *Pelobates syriacus* (Anura, Amphibia) in the early Pleistocene of Italy. Palaeobiodivers. Palaeoenviron. 96, 111–124. https://doi.org/10.1007/s12549-015-0220-1.

Blain, H.-A., Fagoaga, A., Ruiz-Sánchez, F.J., Bisbal-Chinesta, J.F., Delfino, M., 2019. Latest villafranchian climate and landscape reconstructions at Pirro Nord (southern Italy). Geology 47 (9), 829–832. https://doi.org/10.1130/G46392.1.

Blain, H.-A., Fagoaga, A., Ruiz-Sánchez, F.J., García-Medrano, P., Ollé, A., Jiménez-Arenas, J.M., 2021. Coping with arid environments: a critical threshold for human expansion in Europe at the Marine Isotope Stage 12/11 transition? The case of the Iberian Peninsula. J. Hum. Evol. 153, 102950. https://doi.org/10.1016/j.jhevol.2021.102950.

Blain, H.-A., Fagoaga, A., Sánchez-Bandera, C., Ruíz-Sánchez, F.J., Sindaco, R., Delfino, M., 2022. New paleoecological inferences based on the early Pleistocene amphibian and reptile assemblage from Dmanisi (Georgia, Lesser Caucasus). J. Hum. Evol. 162, 103117. https://doi.org/10.1016/j.jhevol.2021.103117.

Böhme, G., Günther, R., 1979. Osteological studies in the European Water Frogs *Rana ridibunda, Rana lessonae* and *Rana "esculenta"* (Anura, Ranidae). Mitt. Zool. Mus. Berlin 55 (1), 203–215.

Carbonell, E., Bermúdez de Castro, J.M., Parés, J.M., Pérez-González, A., Cuenca-Bescós, G., Ollé, A., Mosquera, M., Huguet, R., van der Made, J., Rosas, A., Sala, R., Vallverdú, J., García, N., Granger, D.E., Martinón-Torres, M., Rodríguez, X.P., Stock, G.M., Vergès, J.M., Allué, E., Burjachs, F., Cáceres, I., Canals, A., Benito, A., Díez, C., Lozano, M., Mateos, A., Navazo, M., Rodríguez, J., Rosell, J., Arsuala, J.L., 2008. The first hominin in Europe. Nature 452, 465–469. https://doi.org/10.1038/nature06815.

Cauche, D., 2022. The Vallonnet cave on the northern Mediterranean border: a record of one of the oldest human presences in Europe. L'Anthropologie 126, 102974. https://doi.org/10.1016/j.anthro.2021.102974.

Chao, A., Jost, L., 2012. Coverage-based rarefaction and extrapolation: standardizing samples by completeness rather than size. Ecology 93, 2533–2547. https://doi.org/10.1890/11-1952.1.

Chao, A., Gotelli, N.J., Hsieh, T.C., Sander, E.L., Ma, K.H., Colwell, R.K., Ellison, A.M., 2014. Rarefaction and extrapolation with Hill numbers: a framework for sampling and estimation in species diversity studies. Ecol. Monogr. 84 (1), 45–67. https://doi.org/10.1890/13-0133.

Chao, A., Ma, K.H., Hsieh, T.C., 2016. iNEXT (iNterpolation and EXTrapolation) online: software for interpolation and extrapolation of species diversity. Program and User's Guide published at. http://chao.stat.nthu.edu.tw/wordpress/software_download/.

Cheheb, R.C., Arzarello, M., Arnaud, J., Berto, C., Cáceres, I., Caracausi, S., Colopi, F., Daffara, S., Canini, G.M., Huguet, R., Karambatsou, T., Sala, B., Zambaldi, M., Berruti, G.L.F., 2019. Human behavior and *Homo*-mammal interactions at the first European peopling: new evidence from the Pirro Nord site (Apricena, Southern Italy). Sci. Nat. 106, 16. https://doi.org/10.1007/s00114-019-1610-4.

Chesi, F., Delfino, M., Abazzi, L., Carboni, S., Lecca, L., Rook, L., 2007. New fossil vertebrate remains from San Giovanni di Sinis (Late Pleistocene, Sardinia): the last *Mauremys* (Reptilia, Testudines) in the central Mediterranean. Riv. Ital. Paleontol. Stratigr. 113, 287–297. https://doi.org/10.13130/2039-4942/5875.

Colwell, R.K., Chao, A., Gotelli, N.J., Lin, S.-Y., Mao, C.X., Chazdon, R.L., Longino, J.T., 2012. Models and estimators linking individual-based and sample-based rarefaction, extrapolation and comparison of assemblages. J. Plant Ecol. 5, 3–21. https://doi.org/10.1093/jpe/rtr044.

Correggiari, A., Roveri, M., Trincardi, F., 1996. Late Pleistocene and Holocene evolution of the North Adriatic Sea. Il Quat. 9 (2), 697–704.

Cuenca-Bescós, G., Rofes, J., García-Pimienta, J., 2005. Environmental change across the Early-Middle Pleistocene transition: small mammalian evidence from the Trinchera Dolina cave, Atapuerca, Spain. In: Head, M.J., Gibbard, P.L. (Eds.), Early-Middle Pleistocene Transitions: the land-ocean Evidence, vol. 247. Special Publications, Geol. Soc., London, pp. 277–286. https://doi.org/10.1144/gsl.sp.2005.247.01.16.

Cuenca-Bescós, G., Rofes, J., López-García, J.M., Blain, H.-A., Rabal-Garcés, R., Sauqué, V., Arsuaga, J.L., Bermúdez de Castro, J.M., Carbonell, E., 2013. The small mammals of Sima del Elefante (Atapuerca, Spain) and the first evidence of *Homo* in western Europe. Quat. Int. 295, 28–35. https://doi.org/10.1016/j.quaint.2011.12.012.

Curran, S.C., Drăguşin, V., Pobiner, B., Pante, M., Hellstrom, J., Woodhead, J., Croitor, R., Doboş, A., Gogol, S.E., Ersek, V., Keevil, T.L., Petculescu, A., Popescu, A., Robinson, C., Werdelin, L., Terhune, C., 2025. Hominin presence in Eurasia by at least 1.95 million years ago. Nat. Commun. 16, 836. https://doi.org/10.1038/s41467-025-56154-9.

De Giuli, F., Masini, F., Torre, D., 1986. The earliest Villafranchian faunas in Italy: the Pirro Nord Fauna (Apricena, Gargano). Palaeontogr. ital. 73 116–128.

Delfino, M., 1996. Erpetofauna Tardo Villafranchiana di Cava Dell'Erba e Cava Pirro (Foggia, Puglia, Italia) [undergraduate thesis]: Turin. University di Turin, p. 194.

Delfino, M., 1997. *Blanus* from the early Pleistocene of Southern Italy: another small tessera from a big mosaic. In: Böhme, W., Bischoff, W., Ziegler, T. (Eds.), Herpetologica Bonnensis, pp. 89–97.

Delfino, M., Bailon, S., 2000. Early Pleistocene herpetofauna from cava Dell'Erba and cava Pirro (Apulia, Southern Italy). Herpetol. J. 10, 95–110.

Delfino, M., Atzori, M., 2013. An update on the Early Pleistocene herpetofauna from Pirro Nord. Palaeontograph. Abteilung: Paläozoologie–Stratigraphie 298, 19–29. https://doi.org/10.1127/pala/298/2013/19.

deMenocal, P.B., 2011. Climate and human evolution. Science 331 (6017), 540–542. https://doi.org/10.1126/science.1190683.

Despriée, J., Moncel, M.-H., Arzarello, M., Courcimault, G., Voinchet, P., Bahain, J.-J., Falguères, C., 2018. The 1-million-year-old quartz assemblage from Pont-du-Lavaud (Centre, France) in the European context. J. Quat. Sci. 33, 639–661. https://doi.org/10.1002/jqs.3042.

Domínguez-García, A.C., López-García, J.M., Núñez-Lahuerta, C., Galán, J., Cuenca-Bescós, G., 2024. Palaeoclimatic analysis of Quaternary terrestrial small mammal assemblages from the Sierra de Atapuerca (Burgos, Spain). Palaeogeogr. Palaeoclimatol. Palaeoecol. 655, 112532. https://doi.org/10.1016/j.palaeo.2024.112532.

Duval, M., Falguères, C., Bahain, J.J., Grün, R., Shao, Q., Aubert, M., Hellstrom, J., Dolo, J.M., Agustí, J., Martínez-Navarro, B., Palmqvist, P., Toro-Moyano, I., 2011. The challenge of dating early Pleistocene fossil teeth by the combined uranium series – electron spin resonance method: the Venta Micena palaeontological site (Orce, Spain). J. Quat. Sci. 26 (6), 603–615. https://doi.org/10.1002/jqs.1476.

Duval, M., Falguères, C., Bahain, J.J., Grün, R., Shao, Q., Aubert, M., Toro-Moyano, I., 2012. On the limits of using combined U-series/ESR method to date fossil teeth from two early Pleistocene archaeological sites of the Orce area (Guadix-Baza basin, Spain). Quat. Res. 77 (3), 482–491. https://doi.org/10.1016/j.yqres.2012.01.003.

Duval, M., Arnold, L.J., Bahain, J.-J., Parés, J.M., Demuro, M., Falguères, C., Shao, Q., Voinchet, P., Arnaud, J., Berto, C., Berruti, G.L.F., Daffara, S., Sala, B., Arzarello, M., 2024. Re-examining the earliest evidence of human presence in western Europe: new dating results from Pirro Nord (Italy). Quat. Geochronol. 82, 10519. https://doi.org/10.1016/j.quageo.2024.101519.

Fagoaga, A., Blain, H.-A., Marquina-Blasco, R., Laplana, C., Sillero, N., Hernández, C.M., Mallol, C., Galván, B., Ruiz-Sánchez, F.J., 2019. Improving the accuracy of small vertebrate-based paleoclimatic reconstructions derived from the Mutual Ecogeographic Range. A case study using geographic information systems and UDA-ODA discrimination methodology. Quat. Sci. Rev. 223, 1–12. https://doi.org/10.1016/j.quascirev.2019.105969.

Fagoaga, A., Fernández-García, M., López-García, J.M., Chacón, M.G., Saladié, P., Vallverdú, J., Ruiz-Sánchez, F.J., Blain, H.-A., 2023. Redefining the MIS 3 climatic scenario for Neanderthals in northeastern Iberia: a multi-method approach. Quat. Sci. Rev. 313, 108186. https://doi.org/10.1016/j.quascirev.2023.108186.

Fick, S.E., Hijmans, R.J., 2017. WorldClim 2: new 1km spatial resolution climate surfaces for global land areas. Int. J. Climatol. 37 (12), 4302–4315. https://doi.org/10.1002/joc.5086.

Foister, T., Žliobaitė, I., Wilson, O.E., Fortelius, M., Tallavaara, M., 2023. Homo heterogenus: variability in early Pleistocene *Homo* environments. Evol. Anthropol. Issues News Rev. https://doi.org/10.1002/evan.22005.

Foister, T., Liu, L., Saarinen, J., Tallavaara, M., Zhang, H., Žliobaitė, I., 2024. Quantifying heterogeneity of hominin environments in and out of Africa using herbivore dental traits. Quat. Sci. Rev. 337, 108791. https://doi.org/10.1016/j.quascirev.2024.108791.

Fritz, U., Ayaz, D., Buschbom, J., Kami, H.G., Mazanaeva, L.-F.-, Aloufi, A.A., Auer, M., Rifai, L., Šilić, T., Hundsdörfer, A.K., 2008. Go east: phylogeographies of *Mauremys caspica* and *M. rivulata*–discordance of morphology, mitochondrial and nuclear genomic markers and rare hybridization. J. Evol. Biol. 21, 527–540. https://doi.org/10.1111/j.1420-9101.2007.01485.x.

Gabunia, L., Vekua, A., Lordkipanidze, D., Swisher III, C.C., Ferring, R., Justus, A., Nioradze, M., Tvalchrelidze, M., Antón, S.C., Bosinski, G., Jöris, O., de Lumley, M.-A., Majsuradze, G., Mouskhelishvili, A., 2000. Earliest Pleistocene hominid cranial remains from Dmanisi, Republic of Georgia: taxonomy, geological setting, and age. Science 288, 1019–1025. https://doi.org/10.1126/science.288.5468.101.

Garba, R., Usyk, V., Ylä-Mella, L., Kameník, J., Stübner, K., Lachner, J., Rugal, G., Veselovský, F., Garasimenko, N., Herries, A.I.R., Kučera, J., Knudsen, M.F., Jansen, J.D., 2024. East-to-west human dispersal into Europe 1.4 million years ago. Nature 627, 805–810. https://doi.org/10.1038/s41586-024-07151-3.

Giusti, D., Arzarello, M., 2016. The need for a taphonomic perspective in spatial analysis: formation processes at the Early Pleistocene site of Pirro Nord (P13), Apricena, Italy. JASREP 8, 235–249. https://doi.org/10.1016/j.jasrep.2016.06.014.

Gliozzi, E., Abbazi, L., Argenti, P., Azzaroli, A., Caloi, L., Capasso Barbato, L., Di Stefano, G., Esu, D., Ficcarelli, G., Girotti, O., Kotsakis, T., Masini, F., Mazza, P., Mezzabotta, C., Palombo, M.R., Petronio, C., Rook, L., Sala, B., Sardella, R., Zenalda, E., Torre, D., 1997. Biochronology of selected mammals, molluscs and ostracods from the Middle Pliocene to the late Pleistocene in Italy. The state of the art. Riv. Ital. Paleontol. Stratigr. 103 (3), 369–388. https://doi.org/10.13130/2039-4942/5299.

Greenacre, M.J., 2010. Correspondence analysis. WIREs Computational Statistics 2 (5), 613–619. https://doi.org/10.1002/wics.114.

Hammer, Ø., Harper, D.A.T., Ryan, P.D., 2001. PAST: paleontological statistics software package for education and data analysis. Palaeontol. Electron. 4, 1–9.

Huguet, R., Rodríguez-Álvarez, X.P., Martinón-Torres, M., Vallverdú, J., López-García, J. M., Lozano, M., Terradillos-Bernal, M., Expósito, I., Ollé, A., Santos, E., Saladié, P., de Lombera-Hermida, A., Moreno-Ribas, E., Martín-Francés, L., Allué, E., Núñez-Lahuerta, C., van der Made, J., Galán, J., Blain, H.-A., Cáceres, I., Rodríguez-Hidalgo, A., Bargalló, A., Mosquera, M., Parés, J.M., Pineda, A., Lordkipanidze, D., Margveslashvili, A., Arsuaga, J.L., Carbonell, E., Bermúdez de Castro, J.M., 2025. The earliest face of Western Europe. Nature 640, 707–713. https://doi.org/10.1038/s41586-025-08681-0.

Jackson, S.T., Overpeck, J.T., 2000. Responses of plant populations and communities to environmental changes of the late Quaternary. Paleobiology 26 (S4), 194–220. https://doi.org/10.1666/0094-8373(2000)26[194:roppac]2.0.co2.

Jackson, S.T., Williams, J.W., 2004. Modern analogs in Quaternary paleoecology: here today, gone yesterday, gone tomorrow? Ann. Rev. Earth Planet. Sci. 32, 495–537. https://doi.org/10.1146/annurev.earth.32.101802.120435.

Karampatsou, T., 2017. New Data on Stratigraphy and Formation Processes from Pirro 13 of Pirro Nord (Apulia, Italy).

Lanza, B., Andreone, F., Bologna, M.A., Corti, C., Razzetti, E., 2007. In: Amphibia, X.L.I.I. (Ed.), Fauna D'Italia, Calderini.

Leroy, S.A.G., Ravazzi, C., 1997. Volume of Abstracts and Excursion Guide for the Inter-INQUA Colloquium, 29 March-1 April 1997 on Milankovitch and Plio-Pleistocene Vegetation Successions. Published by INQUA, Milano.

Leroy, S., Arpe, K., Mikolajewicz, V., 2011. Vegetation context and climatic limits of the Early Pleistocene hominin dispersal in Europe. Quat. Sci. Rev. 30, 1448–1463. https://doi.org/10.1016/j.quascirev.2010.01.017.

Lisiecki, L.E., Raymo, M., 2005. A Pliocene-Pleistocene stack of 57 globally distributed benthic δ18O records. Paleoceanogr. Paleoclimatol. 20, PA1003. https://doi.org/10.1029/2004PA001071.

Lona, F., Bertoldi, R., 1973. La storia del Plio-Pleistocene italiano in alcune sequenze vegetazionali lacustri e marine. Memorie Accademica Nazionale Lincei 8 (11), 1–35.

López-García, J.M., Luzi, E., Berto, C., Peretto, C., Arzarello, M., 2015. Chronological context of the first hominin occurrence in southern Europe: the *Allophaiomys ruffoi* (Arvicolinae, Rodentia, Mammalia) from Pirro 13 (Pirro Nord, Apulia, southwestern Italy). Quat. Sci. Rev. 107, 260–266. https://doi.org/10.1016/j.quascirev.2014.10.029.

Marquina-Blasco, R., Fagoaga, A., Crespo, V.D., Bailon, S., Mallol, C., Hernández, C.M., Galván, B., Blain, H.-A., Ruiz-Sánchez, F.J., 2022. Applying the UDA-ODA discrimination technique to a herpetological association: the case of the Middle Palaeolithic site of El Salt (Alcoi, Spain). Archaeol. Antrhopol. Sci. 14 (7), 139. https://doi.org/10.1007/s12520-022-01604-4.

Margari, V., Hodell, D.A., Parfitt, S.A., Ashton, N.M., Grimalt, J.O., Kim, H., Yun, K.-S., Gibbard, P.L., Stringer, C.B., Timmermann, A., Tzedakis, P.C., 2023. Extreme glacial cooling likely led to hominin depopulation of Europe in the Early Pleistocene. Science 381 (6658), 693–699. https://doi.org/10.1126/science.adf4445.

Masini, F., Sala, B., 2007. Large- and small-mammal distribution patterns and chronostratigraphic boundaries from the Late Pliocene to the Middle Pleistocene of the Italian peninsula. Quat. Int. 160, 43–56. https://doi.org/10.1016/j.quaint.2006.09.008.

Masini, F., Sala, B., 2011. Considerations on an integrated biochronological scale of Italian Quaternary continental mammals. Il Quat. 24, 193–198.

Mateo, J.A., 1988. Estudio Sistemático Y Zoogeográfico De Los Lagardos Ocelados *Lacerta Lepida* Daudin, 1802 Y *Lacerta Pater* Lataste, vol. 1880. Unpublished Ph.D Thesis, Universidad de Sevilla.

Mateo, J.A., López-Jurado, L.F., 1997. Dental ontogeny in *Lacerta lepida* (Sauria, Lacertidae) and its relationship to diet. Copeia 1997 (2), 461–463. https://doi.org/10.2307/1447773.

Mondanaro, A., Melchionna, M., Di Febbraro, M., Castiglione, S., Hold A en, P.B., Edwards, N.R., Carotenuto, F., Maiorano, L., Modafferi, M., Serio, C., Diniz-Filho, J. A.F., Rangel, T., Rook, L., O'Higgins, P., Spikins, P., Profico, A., Raia, P., 2020. A major change in rate of climate niche envelope evolution during hominid history. iScience 23, 101693. https://doi.org/10.1016/j.isci.2020.101693.

Muñoz-Delgado, M.C., 2003. Geografía (2° De Bachillerato), p. 431.

Ochando, J., Carrión, J., Altolaguirre, Y., Manuera, M., Amorós, G., Jiménez-Moreno, G., Solano-García, J., Barsky, D., Luzón, C., Sánchez-Bandera, C., Serrano-Ramos, A., Toro-Moyano, I., Saarinen, J., Blain, H.-A., Bocherens, H., Oms, O., Agustí, J., Fortelius, M., Jiménez-Arenas, J.M., 2022. Palynological investigations in the Orce Archaeological Zone, early Pleistocene of Southern Spain. Rev. Palaeobot. Palynol. 304, 104725. https://doi.org/10.1016/j.revpalbo.2022.104725.

Pavia, M., Zunino, M., Coltorti, M., Angelone, C., Arzarello, M., Bagnus, C., Bellucci, L., Colombero, S., Marcolini, F., Peretto, C., Petronio, C., Petrucci, M., Pieruccini, P., Sardella, R., Tema, E., Villier, B., Pavia, G., 2012. Stratigraphical and palaeontological data from the Early Pleistocene Pirro 10 site of Pirro Nord (Puglia, south eastern Italy). Quat. Int. 267, 40–55. https://doi.org/10.1016/j.quaint.2010.12.019.

Pleguezuelos, J.M., Márquez, R., Lizana, M., 2002. Atlas y Libro Rojo de los Anfibios y Reptiles de España. Dirección General De La Conservación De La naturaleza-Asociación Herpetológica Española.

Potts, R., 1998. Environmental hypotheses of hominin evolution. Yearbk. Phys. Anthropol. 41, 93–136. https://doi.org/10.1002/(SICI)1096-8644(1998)107:27+<93::AID-AJPA5>3.0.CO;2-X.

Potts, R., 2002. Complexity and adaptability in human evolution. In: Goodman, M., Moffat, A.S. (Eds.), Probing Human Origins. American Academy of Arts and Sciences, pp. 33–58.

Potts, R., Dommain, R., Moerman, J.W., Beherensmeyer, A.K., Deino, A.L., Riedl, S., Beverly, E.J., Brown, E.T., Deocampo, D., Kinyanjui, R., Lupien, R., Owen, R.B., Rabideaux, N., Russel, J.M., Stockhecke, M., Demenocal, P., Faith, J.T., Garcin, Y., Noren, A., Scott, J.J., Western, D., Bright, J., Clark, J.B., Cohen, A.S., Keller, C.B., King, J., Levin, N.E., Shannon, K.B., Muiruri, V., Renaut, R.W., Rucina, S.M., Uno, K., 2020. Increased ecological resource variability during a critical transition in hominin evolution. Sci. Adv. 6 (43), eabc8975. https://doi.org/10.1126/sciadv.abc8975.

Ramírez-Pedraza, I., Tornero, C., Aouraghe, H., Rivals, F., Patalano, R., Haddoumi, H., Expósito, I., Rodríguez-Hidalgo, A., Mischke, S., van der Made, J., Piñero, P., Blain, H.-A., Roberts, P., Jha, D.K., Agustí, J., Sánchez-Bandera, C., Lemjidi, A., Benito-Calvo, A., Moreno-Ribas, E., Oujaa, A., Mhamdi, H., Souhir, M., Aissa, A.M., Chacón, M.G., Sala-Ramos, R., 2024. Arid, mosaic environments during the Plio-Pleistocene transition and early hominin dispersals in northern Africa. Nat. Commun. 15, 8393. https://doi.org/10.1038/s41467-024-52672-0.

Roček, Z., 1980. Intraspecific and ontogenetic variation of the dentition in the green lizard *Lacerta viridis* (Reptilia, Squamata). Vest. cs. Spolec. zool. 44, 272–277.

Saarinen, J., Oksanen, O., Žliobaitė, I., Fortelius, M., de Miguel, D., Azanza, B., Bocherens, H., Luzón, C., Yravedra, J., Courtenay, L.A., Blain, H.-A., Sánchez-Bandera, C., Serrano-Ramos, A., Rodríguez-Alba, J., Viranta, S., Barsky, D., Solano-García, J., Tallavaara, M., Oms, O., Agustí, J., Jiménez-Arenas, J.M., 2021. Pliocene to Middle Pleistocene climate history in the Guadix-Baza Basin, and the environmental conditions of early human dispersal into Europe. Quat. Sci. Rev. 268, 107132. https://doi.org/10.1016/j.quascirev.2021.107132.

Sala, B., Masini, F., 2007. Late Pliocene and Pleistocene small mammal chronology in the Italian Peninsula. Quat. Int. 160, 4–16. https://doi.org/10.1016/j.quaint.2006.10.002.

Sánchez-Bandera, C., Oms, O., Blain, H.-A., Lozano-Fernández, I., Bisbal-Chinesta, J.F., Agustí, J., Saarinen, J., Fortelius, M., Titton, S., Serrano-Ramos, A., Luzón, C., Solano-García, J., Barsky, D., Jiménez-Arenas, J.M., 2020. New stratigraphically constrained palaeoenvironmental reconstructions for the first human settlement in Western Europe: the Early Pleistocene herpetofaunal assemblages from Barranco León and Fuente Nueva 3 (Granada, SE Spain). Quat. Sci. Rev. 243, 106466. https://doi.org/10.1016/j.quascirev.2020.106466.

Sánchez-Bandera, C., Fagoaga, A., Serrano-Ramos, A., Solano-García, J., Barsky, D., DeMiguel, D., Ochando, J., Saarinen, J., Piñero, P., Lozano-Fernández, I., Courtenay, L.A., Titton, S., Luzón, C., Bocherens, H., Yravedra, J., Fortelius, M., Agustí, J., Carrión, J.S., Oms, O., Blain, H.-A., Jiménez-Arenas, J.M., 2023. Glacial/interglacial climate variability in southern Spain in the late early Pleistocene and climate backdrop for early *Homo* in Europe. Palaeogeogr. Palaeoclimatol. Palaeoecol. 625, 111688. https://doi.org/10.1016/j.palaeo.2023.111688.

Sánchez-Bandera, C., Blain, H.-A., Bisbal-Chinesta, J.F., Fagoaga, A., Pavia, M., Delfino, M., 2025. Replication data for: new palaeoecological insights for the early human occupation in Europe: amphibians and reptiles from the Early Pleistocene of Pirro Nord 13 (Apricena, southern Italy). CORA. Repositori de Dades de Recerca V1. https://doi.org/10.34810/data2091.

Sánchez-Vialas, A., Buckley, D., Recuero, E., Martínez-Freiría, F., Velo-Antón, G., Bisbal-Chinesta, J.F., Martínez-Solano, Í., 2024. Species list of the Spanish herpetofauna: an uptade. Basic and Applied Herpetology 38, 5–23.

Sillero, N., Campos, J., Bonardi, A., Corti, C., Creemers, R., Crochet, P.-A., Isalović, J.C., Denoël, M., Ficetola, G.F., Gonçalves, J., Kuzmin, S., Lymberakis, P., de Pous, P., Rodríguez, A., Sindaco, R., Speybroeck, J., Toxopeus, B., Vieites, D.R., Vences, M.,

2014. Updated distribution and biogeography of amphibians and reptiles of Europe. Amphibia-Reptilia 35, 1–30. https://doi.org/10.1163/15685381-00002935.
Sindaco, R., Doria, G., Razzetti, E., Salvidio, S. (Eds.), 2009. Atlante Degli Anfibi E Dei Rettili D'Italia/Atlas of Italian Amphibians and Reptile, second ed. Edizioni Polistampa, Florence, Italy, Societas Herpetologica Italiana, p. 729.
Sindaco, R., Kornilios, P., Sacchi, R., Lymberakis, P., 2014. Taxonomic reassessment of *Blanus strauchi* (Bedriaga, 1884) (Squamata: Amphisbaenia: Blanidae), with the description of a new species from south-east Anatolia (Turkey). Zootaxa 3795, 311–326. https://doi.org/10.11646/zootaxa.3795.3.6.
Sokal, R.R., Rohlf, F.J., 1962. The comparison of dendrograms by objective methods. Taxon 11 (2), 33–40. https://doi.org/10.2307/1217208.
Speybroeck, J., Beukema, W., Dufresnes, C., Fritz, U., Jablonski, D., Lymberakis, P., Martínez-Solano, I., Razzetti, E., Vamberger, M., Vences, M., Vörös, J., Crochet, P.-A., 2020. Species list of the European herpetofauna – 2020 update by the Taxonomic Committee of the Societas Europaea Herpetologica. Amphibia-Reptilia 41, 139–189. https://doi.org/10.1163/15685381-bja10010.
Szyndlar, Z., 1984. Fossil snakes from Poland. Acta Zool. Cracov. 28, 1–156.
Szyndlar, Z., 1991. A review of Neogene and Quaternary snakes of Central and Eastern Europe. Part I: scolecophidia, Boidae, Colubrinae. Estudios geológicos 47 (1–2), 103–126. https://doi.org/10.3989/egeol.91471-2412.
Timmermann, A., Yun, K.-S., Raia, P., Ruan, J., Mondanaro, A., Zeller, E., Zollikofer, C., Ponce de León, M., Lemmon, D., Willeit, M., Ganopolski, A., 2022. Climate effects on archaic human habitats and species successions. Nature 604, 495–501. https://doi.org/10.1038/s41586-022-04600-9.
Timmermann, A., Raia, P., Mondanaro, A., Zollikofer, C.P.E., Ponce de León, M., Zeller, E., Yun, K.-S., 2024. Past climate change effects on human evolution. Nat. Rev. Earth Environ. 5, 701–716. https://doi.org/10.1038/s43017-024-00584-4.
Toro-Moyano, I., Martínez-Navarro, B., Agustí, J., Souday, C., Bermúdez de Castro, J.M., Martinón-Torres, M., Fajardo, B., Duval, M., Falguères, C., Oms, O., Maria Parés, J., Anadón, P., Julià, R., García-Aguilar, J.M., Moigne, A.-M., Espigares, M.P., Ros-Montoya, S., Palmqvist, P., 2013. The oldest human fossil in Europe, from Orce (Spain). J. Hum. Evol. 65 (1), 1–9. https://doi.org/10.1016/j.jhevol.2013.01.012.
Velo-Antón, G., Pinya, S., 2015. El galápago leproso (*Mauremys leprosa*) en la Península Ibérica e Islas Baleares. Bol. Asoc. Herpetol. Espanola 26 (2), 39–42.
Vialet, A., Prat, S., Wils, P., Alçiçek, M.C., 2018. The Kocabaş hominin (Denizli Basin, Turkey) at the crossroads of Eurasia: new insights from morphometric and cladistics analyses. C. R. - Palevol 17 (1–2), 17–32. https://doi.org/10.1016/j.crpv.2017.11.003.
Villa, A., Delfino, M., 2019. A comparative atlas of the cranial osteology of European lizards (Reptilia, Squamata). Zool. J. Linn. Soc. 187, 828–928. https://doi.org/10.1093/zoolinnean/zlz035.
Villa, A., Kirchner, M., Alba, D.M., Bernardini, F., Bolet, A., Luján, À.H., Fortuny, J., Hipsley, C.H., Müller, J., Sindaco, R., Tuniz, C., Delfino, M., 2019. Comparative cranial osteology of *Blanus*(Squamata: Amphisbaenia). Zool. J. Linn. Soc. 185 (3), 693–716. https://doi.org/10.1093/zoolinnean/zly082.
Yeshurun, R., Lev, M., Edeltin, L., Amos, L., Orbach, M., Lavy-Elbaz, S., Ujma, C., Wieler, N., Marder, O., 2024. The early Natufian site of Hof shahaf, Israel: subsistence, environment, and settlement dynamics. J. Paleo. Arch. 7, 33. https://doi.org/10.1007/s41982-024-00200-3.
Zeller, E., Timmermann, A., Yun, K.-S., Raia, P., Stein, K., Ruan, J., 2023. Human adaptation to diverse biomes over the past 3 million years. Science 380 (6645), 604–608. https://doi.org/10.1126/science.abq1288.